THESIS

DEVELOPMENT OF PREDICTIVE ENERGY MANAGEMENT STRATEGIES FOR HYBRID ELECTRIC VEHICLES

Submitted by

David Baker

Department of Mechanical Engineering

In partial fulfillment of the requirements

For the degree of Master of Science

Colorado State University

Fort Collins, Colorado

Fall 2017

Master's Committee:

Advisor: Thomas H. Bradley

John Petro
Peter Young

ABSTRACT

DEVELOPMENT OF PREDICTIVE ENERGY MANAGEMENT STRATEGIES FOR HYBRID ELECTRIC VEHICLES

Studies have shown that obtaining and utilizing information about the future state of vehicles can improve vehicle fuel economy (FE). However, there has been a lack of research into the impact of real-world prediction error on FE improvements, and whether near-term technologies can be utilized to improve FE. This study seeks to research the effect of prediction error on FE. First, a speed prediction method is developed, and trained with real-world driving data gathered only from the subject vehicle (a *local* data collection method). This speed prediction method informs a predictive powertrain controller to determine the optimal engine operation for various prediction durations. The optimal engine operation is input into a high-fidelity model of the FE of a Toyota Prius. A tradeoff analysis between prediction duration and prediction fidelity was completed to determine what duration of prediction resulted in the largest FE improvement. Results demonstrate that 60-90 second predictions resulted in the highest FE improvement over the baseline, achieving up to a 4.8% FE increase. A second speed prediction method utilizing simulated vehicle-to-vehicle (V2V) communication was developed to understand if incorporating near-term technologies could be utilized to further improve prediction fidelity. This prediction method produced lower variation in speed prediction error, and was able to realize a larger FE improvement over the local prediction method for longer prediction durations, achieving up to 6% FE improvement. This study concludes that speed prediction and prediction-informed optimal vehicle energy management can produce FE improvements with real-world prediction error and drive cycle variability, as up to 85% of the FE benefit of perfect speed prediction was achieved with the proposed prediction methods.

ACKNOWLEDGEMENTS

I would like to thank my advisor, Dr. Thomas Bradley, for all the support, patience, valuable insight and multitude of great ideas that he supplied me with. I am very grateful for how much he has helped me grow academically, professionally and personally during this endeavor.

I would also like to thank all of my friends and family for supporting me during my Master's studies, and for all of the proofreading everyone painstakingly took part in on my behalf.

TABLE OF CONTENTS

LIST OF TABLES

LIST OF FIGURES

1. INTRODUCTION

1.1 LITERATURE REVIEW

The fact that the climate is changing is well understood and acknowledged. The burning of fossil fuels is generally accepted as one of the largest contributors to climate change and poor air quality. The International Energy Agency has determined that of the CO_2 produced from burning fuels across the world, 23% is emitted from the transportation sector [1]. Of the petroleum fuel used and greenhouse gases (GHG) emitted in the transportation sector, 60% is from light duty vehicles [2]. To minimize the effects of climate change, most of the countries in the world have agreed to the Paris Climate Agreement, which aims to keep global warming under 2 °C [3]. Increasingly strict fuel economy and GHG emissions regulations have proven to be one of the most efficient policy tools for improving fuel economy [4]. The United States Environmental Protection Agency and National Highway Traffic Safety Administration have implemented Corporate Average Fuel Economy (CAFE) standards that automakers are required to meet. By 2025, the minimum standard for domestically manufactured passenger cars will be 51.3 MPG [5]. These standards allow automakers freedom to determine which technologies they utilize to reach the required fuel economy and GHG emissions standards.

Many studies have concluded that hybrid electric vehicles (HEV) and plug-in hybrid electric vehicles (PHEV) are the best means to improving near-term sustainability and vehicle FE [6]–[8]. Sales of HEVs and PHEVs are increasing in the U.S., as well as globally [7], [9]. However, PHEVs and electric vehicles are still in the "early adopter" stage of market penetration [10]. The FE of hybrid vehicles is strongly influenced by their energy management strategies (EMS) [11]. Since hybrid vehicles have two power sources (typically an internal combustion engine and an electric

motor), there is more freedom in determining how to fulfil the driver's power request. Optimizing the EMS is a crucial aspect of increasing FE, and is a very active area of research today.

To achieve optimal EMS, it is necessary for vehicles to shift from the current, reactive EMS, towards predictive EMS that can take into account the power needs of the vehicle in the future [12]. The continuous, incremental integration of advanced driver assistance systems (ADAS) and intelligent transportation systems (ITS) is making it possible to shift towards predictive energy management, and higher FE.

Implementation of ADAS into vehicles is generally split into two main categories: improving FE via driving modification and improving FE without driving modification. Driving modification is accomplished through either modifying the route of travel (eco-routing) [13] or by modifying the driving characteristics, such as traveling at most efficient speeds, and with less aggressive acceleration/decelerations (eco-driving). This study, however, focuses on optimal energy management via powertrain control, without changing the responsiveness or dynamics of the vehicle.

There are two main considerations for using ADAS and ITS for optimal EMS: 1) obtaining future information, and 2) utilizing that information to achieve optimal (or near optimal) energy management. Relevant future information that is desired to be known are things such as future vehicle speed, road grade, road speed limits, traffic signals, traffic flow and density. Some of the technologies that are either currently available, or are expected to be available in the near future, would include GPS location, geographic information system (GIS) information, vehicle-to-vehicle communication and vehicle-to-infrastructure (V2I) communication. GPS information is currently available on most cars today, GIS information is not readily on cars today, but the information is available on off-vehicle networks. V2V and V2I communication is not commercially available.

However, many researchers assume one or both of V2V or V2I technologies are available in their method of obtaining future information [14]–[16]. The intention of this study is to not assume that future technology is available and mature, but rather to develop a method of obtaining future information using first, technology that is commercially available today, and next a method of implementing low level V2V information to improve prediction accuracy, in turn further increasing FE.

1.1.1 Neural Networks in Vehicle Speed Predictions

There are a multitude of ways to use these aforementioned technologies to obtain desired information and make predictions from it. In general, all methods obtain certain information and use it to inform a model, which creates the prediction. Relatively recently, there has been a shift away from using analytical models to data-driven, learning-based models for predictions [17]. Data-driven models have the advantage of being flexible, not having prior assumptions associated with the input variables, and being more robust to noisy data [18]. One of the most widely used data-driven models is learning-based Artificial Neural Networks (NN). In general, NNs are useful because of their ability to model nonlinear functions, their flexible model structure, and their ability to handle multi-dimensional data [19].

There is a wide range of types of NNs that are used for predicting vehicle conditions: multi-layer perceptron (MLP NN), radial basis function (RBF NN), long short-term (LST NN), nonlinear autoregressive neural network with exogenous inputs (NARX NN) and chaining neural networks (CNN) [14], [16], [18], [20]–[22]. These types of NNs are all capable of predicting multiple time steps ahead, but have strengths in different applications. MLP NNs have been used in vehicle applications to predict future velocities with only previous velocities as the input [21], to predict future velocities based on V2V signal strength and vehicle distance [22] and to predict speed

reduction and distance from on/off ramps [20]. Radial basis function NNs have been used to predict future velocities based on V2V signal strength and vehicle distance [22] and to predict future velocity sequences based on previous velocity sequences [23]. LSTM NNs and CNNs have been utilized to predict vehicle speeds from V2V and V2I roadside sensors [14], [18]. NARX NNs have the added flexibility that they can use other exogenous inputs in addition to predicting multiple time steps ahead (by feeding the output of one iteration as an input to the next). Valera et al. use NARX NNs to predict the difference between the actual vehicle speed and a pre-calculated expected speed trace [16]. Additionally, other methods of speed prediction, such as Markov chains, [24] have been studied extensively but are not a focus of this research. In this study, an individual vehicle velocity prediction method is developed using a NARX NN, which utilizes the vehicles latitude and longitude as exogenous inputs.

1.1.2 V2V Communication Modeling

V2V communication is not currently commercially available, but researchers are investigating ways to utilize information obtained by V2V to make vehicle speed predictions, as the technology will be commercially available in the near future. Many researchers are assuming that V2V and V2I are both fully available for obtaining detailed vehicle information [14]–[16]. For instance, Valera, *et al.* doesn't even differentiate between V2V and V2I, but just say that this type of technology can be used to integrate dynamic traffic information into their prediction model [16]. The dynamic traffic information they discuss is made up of traffic events, traffic state, weather state, etc. In their simulations, this information was added manually, without detailed discussion of how that information would be obtained. Zhang, *et al.* assume full V2V and V2I communication capabilities are on all cars, that there is a 200m range of communication and that there are no communication errors [14]. Additionally, they assume multiple leading vehicles'

velocities are broadcast to the ego vehicle, along with the leading vehicle's distance to the next stoplight. This all assumes very comprehensive data communication, which is unrealistic for near-term V2V commercial market penetration scenarios. Another study assumes full V2I and V2V communication for a range of 300m where information about vehicles' current and predicted speeds are communicated, as well as traffic speed and density [15]. One study acknowledges there will be a transitional period of implementation of this technology [25], and they devised a way to utilize limited V2V communication penetration into the flow of traffic. However, this method was used to predict the velocity of the vehicle directly in front of the ego vehicle for adaptive cruise control purposes, instead of FE. In the current study, so as to model near-term realizable scenarios and technologies, we assume that there is a limited amount of information being communicated between vehicles: only vehicle speed and GPS location information.

1.1.3 Prediction Error Handling

Vehicle speeds are highly transient, random, and are dependent on many factors such as traffic, road type, weather, driver style, etc. [26]. Vehicle speed predictions are, therefore, bound to have some random and bias errors. There is a range of different procedures for dealing with these errors when investigating speed predictions. There have been instances when researchers did not address prediction errors and used the prediction, without including error, as if it were the actual speed trace [27]. Many acknowledge that the predictions will be erroneous and add different amounts of random error into their "predictions" because error quantification is out of their scope of study [15], [28], [29]. A more realistic way of introducing errors is to use real-world data to derive the speed predictions, which inherently includes realistic errors of both bias and random types [30]–[32]. This method allows for a better understanding of the impact of prediction error and is the method utilized in this study.

1.1.4 Prediction Fidelity Quantification

For quantifying the accuracy of speed predictions, many researchers use simple error calculations such as root mean square error (RMSE) (Eq. 1) or mean absolute percent error (MAPE) (Eq. 2) [14], [18], [21], [22], [33].

$$RMSE = \sqrt{\frac{1}{N}\sum_{j=1}^{N}(y_{pred_j} - y_{act_j})^2} \tag{1}$$

$$MAPE = \frac{100}{N}\sum_{j=1}^{N}\left|\frac{(y_{pred_j} - y_{act_j})}{y_{pred_j}}\right| \tag{2}$$

where N is the total number of observations, y_{pred_j} is the j[th] predicted observation, and y_{act_j} is the j[th] actual observation. However, this might not be provide full insight into the actual accuracy of the prediction. For example, if the prediction is trending very well, but shifted (lagging or ahead) by a short time, then the calculated error will be very high during transient speed situations. However, in terms of fuel economy, that short shift may not have a significant impact on the velocity prediction and the quality of the controls that are derived from it. Thus, a more holistic understanding of the impact of prediction methods and associated error can be gained by using vehicle fuel economy as the metric of comparison [28], [29], [34]. Although, these researchers have performed their analysis based on FE, they did so to understand how prediction error affects the EMS they are using (i.e. adaptive equivalent consumption minimization strategy (A-ECMS), model predictive control (MPC)). To isolate the impact of prediction error, it is necessary to use a global optimal EMS, such as dynamic programming (DP). With a global optimal EMS, the FE performance of a realistic, sub-optimal EMS can then be directly tied to prediction error.

1.1.5 Prediction Duration Tradeoffs

Another consideration for speed prediction that has not been included in many studies is the consideration of the tradeoffs of prediction durations. Logically, as prediction durations become longer, the prediction will be less accurate. Rezaei and Burl investigated prediction horizon length for performance of MPC, but did not consider the impact of prediction errors [33]. He *et al.* considered prediction duration for updating the equivalence factor of the A-ECMS [29]. They considered prediction error, but artificially added it in increments of 0-20% error, for all prediction horizons, thus not considering that prediction error increases with prediction duration. Sun *et al.* also investigated different prediction lengths to update the equivalence factor of an A-ECMS and considered with increasing predictions, there will be more error. They concluded that 60-second prediction horizon was optimal for that application [23]. However, they were investigating how robust the EMS is to prediction error. We seek to isolate the prediction error impacts by investigating the optimal FE that can be derived from real-world predictions, with associated real-world error, and doing a tradeoff analysis of prediction duration and prediction accuracy.

1.1.6 Optimization of EMS

Obtaining future information is only one part of optimal EMS. The second part is the actual energy management strategy that is used. Dynamic programming, as a means of deriving the optimal control for a given state space, is well understood [35] and its application to the optimal HEV energy management is well documented in literature articles [36]–[40] and textbooks [41], [42]. The drawback of dynamic programming is that it is computationally costly and thus difficult to implement in real time for HEV energy management [43]. As a result, research has moved towards more implementable versions of this method such as stochastic dynamic programming [44]–[47], model predictive control [48]–[52] and equivalent consumption minimization strategy

[14], [23], [28], [29], [34]. Because of the difficulties of real-world implementation of dynamic programming, researchers now mainly use it as a convenient (offline calculable) measure of the globally optimal results [32], [53]. Dynamic programming is used in the same way in this study; to understand the impact of prediction error on fuel economy through comparison to the FE of a globally optimal strategy. In the shift to predictive energy management strategies, it is important to understand the robustness of FE gain over reactive energy management strategies (the current state of art). With this understanding, it is then possible to evaluate predictive EMS as derived in real-time.

1.2 RESEARCH QUESTIONS

To summarize the state of the art, uncertainty in prediction defines the tradeoff between fuel economy improvement and prediction horizon duration. As the prediction horizon lengthens, the optimal controller has more predictive data with which realize higher fuel economy, but as the prediction horizon lengthens, the error in prediction grows. This suggests that to define the tradeoff between prediction horizon and fuel economy improvement the uncertainty in each must be quantified and informed using real-world datasets and predictions. However, error quantification, propagation and robust optimization has been given little attention in the studies performed to date.

The results of this literature review leads to three research questions that inform the remainder of this thesis.

1. The quality and quantity of the driving prediction defines the tradeoff between prediction horizon duration and FE. What duration of prediction horizon realizes the largest FE improvement?

2. Are the FE benefits of prediction and optimal EMS robust to real-world variability in prediction error and drive cycles?
3. What level of FE can be realized through leveraging near-term low cost technologies, such as V2V?

1.3 NOVEL ASPECTS OF THIS RESEARCH

This study takes a data-driven, and systems level approach to understanding the impact of real-world prediction error on fuel economy. Two methods are developed to make speed predictions, which focus on current and near-term technology. One only utilizes technology that is commercially available on current vehicles. The other investigates utilizing information that will be exchanged in early stages of V2V communication. Both of these methods utilize real-world driving data, thus prediction errors are representative of real-world prediction errors. Instead of using only standard RMSE quantifications of prediction accuracy, a system level metric of performance (fuel economy) is used.

Through this study, it is intended to understand and quantify the impact of real-world prediction error on potential FE improvements, and to understand if these predictions with real-world error can be used to improve current FE and to conclude if current technology can be incrementally implemented to transition from reactive to predictive energy management.

1.4 THESIS OUTLINE

The structure of the rest of this thesis is outlined in this section. In Chapter 2, we discuss a speed prediction method that involves only local vehicle information that is obtained via technology that is commercially available on vehicles today. We investigate the tradeoffs between prediction horizon lengths and the realizable FE that be derived from this prediction method. In

Chapter 3, we discuss a speed prediction method that incorporates V2V communication. Again, we investigate the tradeoffs between prediction horizon lengths and the realizable FE that be derived from this prediction method. In Chapter 4, we compare the two prediction methods, and then revisit the research questions and draw conclusions from this study in Chapter 5.

2. SPEED PREDICTION METHOD 1: LOCAL VEHICLE DATA

2.1 LOCAL PREDICTION METHODS

Prediction-based EMS aims to maximize fuel economy by predicting the vehicle speed for an upcoming segment of time and optimizing the engine control for that prediction horizon, all in real time. In this portion of the study, speed predictions are made using a NARX NN. To investigate the tradeoff between prediction horizon and the deviation between predicted and actual vehicle speeds (prediction error), a range of prediction horizons is evaluated for their effect on vehicle FE.

The goal of this study is to compare the vehicle FE for differing prediction horizons, to a baseline with no speed prediction, and to an idealized case with perfect speed predictions. These comparisons will allow for a better understanding of the impact of real-world prediction errors on potential FE improvements.

2.1.1 Baseline Vehicle Fuel Economy Modeling

The baseline vehicle controller and vehicle plant model operate on an equation-based algorithm. The vehicle plant and baseline controller are a high-fidelity FE model of a generation three Toyota Prius, previously developed at CSU [32]. Figure 1 shows the general information flow through the baseline controller. A model of a driver receives the velocity trace (velocity vs. time) and outputs a wheel torque request, i.e. the torque that is required at the wheels to propel the vehicle at the desired velocity. The running controller model (sometimes referred to as a hybrid supervisory controller) obtains the wheel torque request from the driver model. Based on the current vehicle states and the desired wheel torque request, the running controller model

determines what the engine, motor and generator torques and speeds should be. The running controller model passes these requests to the vehicle plant model, which simulates the physical components of the vehicle. The vehicle plant model then outputs (among other things) the vehicle speed, ESS SOC and fuel consumed.

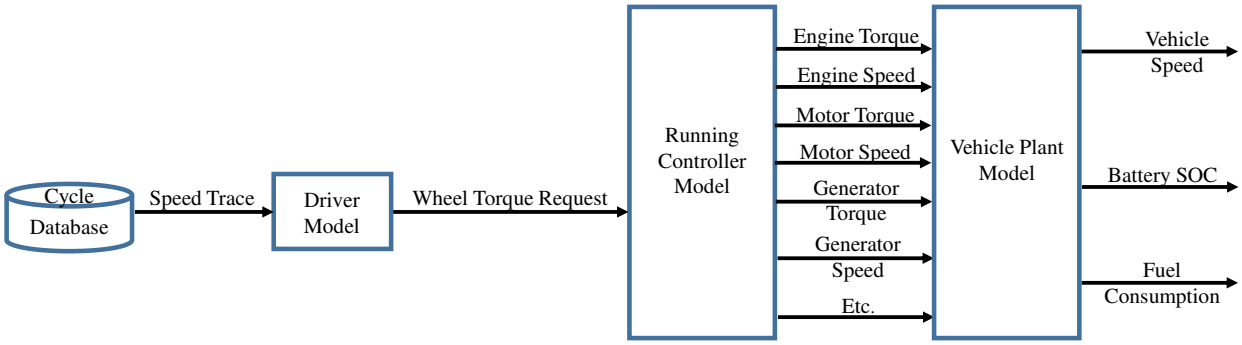

Figure 1: Information flow through baseline FE model of a generation three Toyota Prius

To ensure this model is a valid representation of a generation three Toyota Prius, simulations of three EPA drive cycles are developed. The FE results of these simulations are compared to actual driving data on these drive cycles for a 2010 Toyota Prius [54]. Table 1 demonstrates this comparison. Based on the similarities to real-world FE, the model is considered validated for predicting FE of a real-world Toyota Prius.

Table 1: Comparison of baseline model and experimental FE

	UDDS	HWFET	US06
Experimental	69.6 mpg	67.3 mpg	43.5 mpg
Simulation	71.8 mpg	67.9 mpg	44.0 mpg
Percent Difference	3.2%	0.9%	1.0%

2.1.2 Drive Cycle Development

Existing EPA standard drive cycles aim to capture a mixture of generic city and highway driving. In order to capture a similar mix, through a shortened drive cycle, a custom cycle in Fort Collins, Colorado is developed. A shorter drive cycle is desired because the route needs to be driven multiple times. The route that was developed for this study is shown in Figure 2.

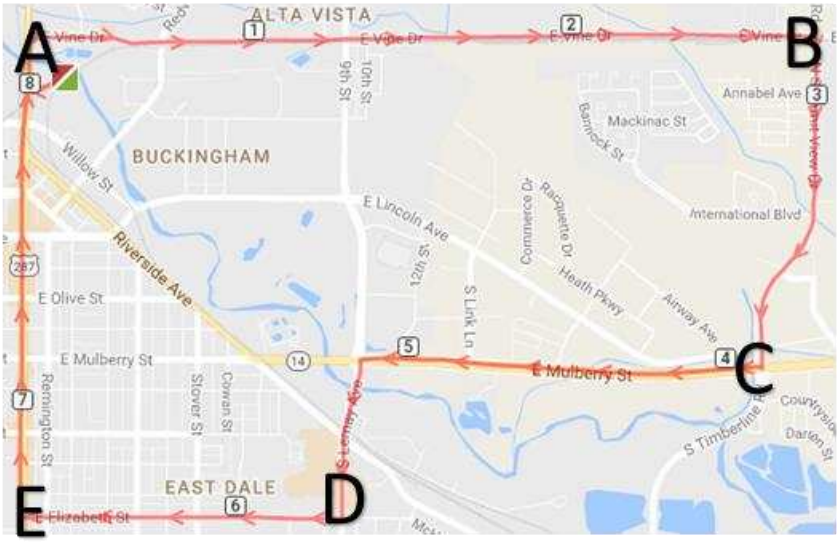

Figure 2: Custom drive cycle route in Fort Collins, CO

Vehicle speed and GPS location are recorded from the Controller Area Network (CAN) bus during each trip along the route. An example speed trace is shown in Figure 3. Note that the letters show points of correspondence between the location shown in Figure 2, and the speed trace shown in Figure 3.

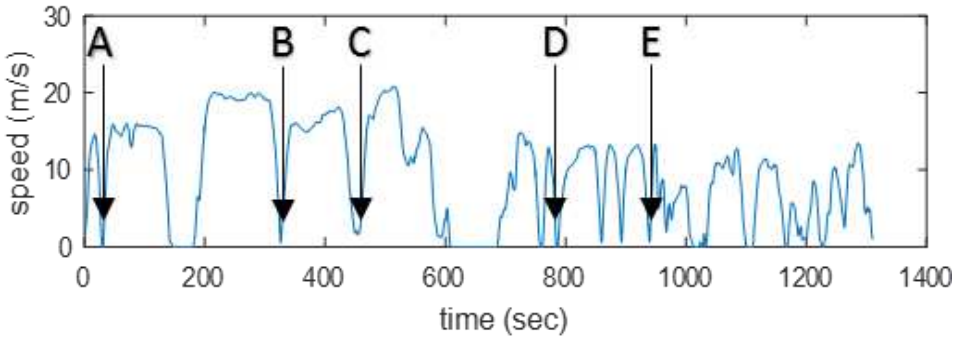

Figure 3: Speed trace of custom drive cycle

To collect data for NARX NN training, this drive cycle is driven 11 times, on different days and at different times of day to capture as much variation as possible. Data from eight of the cycles is used to train, validate and test the NARX NN, and data from the other three are used in the FE simulations. To develop a baseline FE for use as a comparison to speed prediction FE, simulations of the custom drive cycles using the baseline controller were developed. These baseline simulations provide an important baseline comparison for the optimized FE results.

2.1.3 Neural Network Vehicle Speed Predictions

As stated above, a NARX NN is used to make vehicle speed predictions based on current, past and future GPS locations and past vehicle speeds. Since the NARX NNs are trained with actual driving data, these predictions are representative of how the driver drives. Thus, if the driver drives aggressively, the NARX NN will predict aggressive driving behaviors.

The exogenous inputs to the NARX NN are the vehicle's longitude and latitude. It is assumed that knowledge of the route that is being driven is available, thus future GPS locations are available to be used in the NARX NN. The output of the NARX NN is the vehicle speed. Only one hidden layer is used. The architecture of the NARX NN is shown in Figure 4. There was no pre-processing of the data before using it to train the NARX NN.

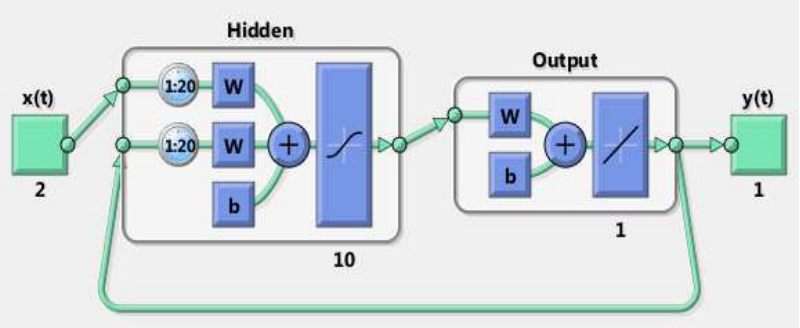

Figure 4: Closed Loop NARX NN [55]

A different NARX NN is defined and trained for each prediction horizon. The method of developing each NARX NN is the same, but the architecture (number of hidden neurons and input delays), and fitted parameters (weights and biases) are different. The general method for developing the NARX NN will be explained, and then the method for determining the architecture and parameters to be used for each NARX NN will be discussed.

The architecture parameters, which are changed for each NARX NN, are prediction horizon length, number of hidden neurons, and number of input and feedback delays. The number of input and feedback delays are set equal to each other for each NARX NN. Each NARX NN only has one hidden layer, uses Levenberg-Marquardt backpropagation to update weights and biases, a hyperbolic tangent sigmoid transfer function for the hidden layer and a linear transfer function for the output layer.

Once the parameters are set for the NARX NN, it is then trained using the entire cycle dataset from the eight drive cycles on an open loop. In a closed loop NARX NN, the output of the current time step is used as an input for the next time step. An open loop differs in that rather than using the output from the previous time step as the input, it uses the actual, known, target value. This makes training of the NARX NN faster and more efficient [55]. Once training is complete, the NARX NN is then closed. The input of vehicle speed is now taken from the output of the NARX

NN from the previous time step. An example of an open loop NARX NN is shown in Figure 5. It can be compared to the closed loop NARX NN depicted in Figure 4.

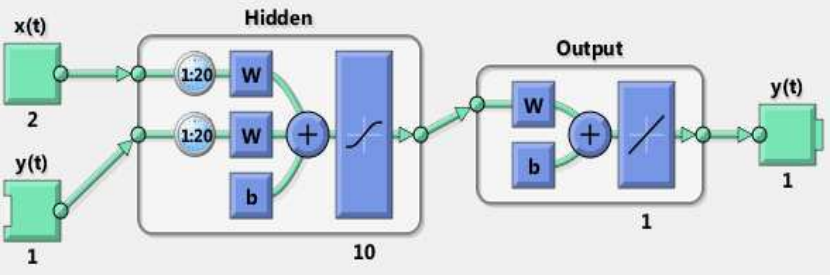

Figure 5: Open Loop NARX NN [55]

To determine the NARX NN parameters for each prediction horizon, many feasible combinations of hidden neurons and delays are used to predict the drive cycle. The range of hidden neurons explored is from 6-16 and delays from 2-26 seconds. The combination that produces the lowest average mean square error, calculated using equation 3 (where where N is the total number of observations, y_{pred_j} is the j[th] predicted observation, and y_{act_j} is the j[th] actual observation), over the entire validation drive cycle (one not used at all in training) is used for that prediction horizon. Once the training is completed, the NARX NN is ready to make vehicle speed predictions for the set prediction horizon.

$$MSE = \frac{1}{N}\sum_{j=1}^{N}(y_{pred_j} - y_{act_j})^2 \tag{3}$$

2.1.4 Development of Predictive Powertrain Controller

A predictive engine controller that was developed in previous research at Colorado State University [32], [53] is leveraged as a foundation in this research to determine optimal engine control based on predicted vehicle speeds. The controller uses dynamic programming to evaluate all possible states and determine the optimal engine power for each state. The states are the SOC

of the ESS and the time over the prediction horizon. The input of the DP algorithm is the speed trace and the output is a table of optimal engine power for all combinations of SOC and time steps. The optimal engine power is found by minimizing the fuel consumed over the prediction horizon. One important constraint of the algorithm is that the SOC at the end of the speed trace is set to be a constant (50%), to simulate a charge-sustaining situation.

2.1.5 Implementation of Prediction and Predictive Powertrain Controller into FE Model

To evaluate the benefit of predicting future vehicle speeds, the prediction and predictive powertrain controller are implemented into the running controller of the FE model so that speed predictions and engine control can be developed as the simulated vehicle is driving. The baseline controller in the model is adapted to have the capability to use the NARX NN to make speed predictions of the upcoming vehicle speed using previous vehicle speed and GPS location. The predicted speed is then input into the predictive powertrain controller to calculate the optimal engine power for each SOC and time for the upcoming prediction horizon.

This routine is repeated at 1 Hz to ensure that the maximum realizable FE potential is achieved. This does not diminish the benefits of having a longer prediction horizons. The DP algorithm in the predictive powertrain controller is run over the entire prediction horizon at each time step, so it determines the optimal engine control for that entire prediction horizon. Repeating this routine at 1 Hz ensures vehicle information is as up to date as possible and this routine is also utilized for the idealized cases of perfect speed predictions. It should be noted that this method differs from making a prediction for the prediction horizon and then using that control for the entire prediction horizon. Figure 6 shows the flow of information between the local prediction algorithm, the predictive powertrain controller, the modified running controller and the vehicle plant model.

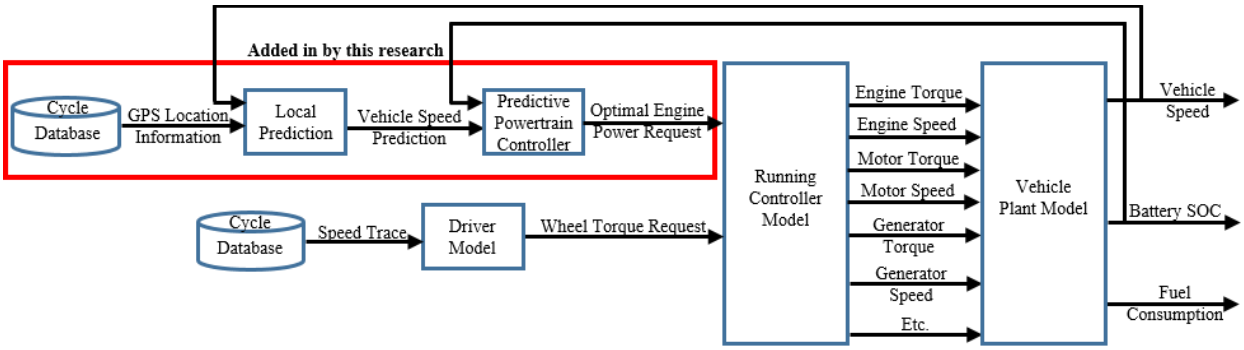

Figure 6: Information flow through FE model, including the local prediction algortihm and predictive powertrain controller

Vehicle speed as a function of time is input into the driver model from the drive cycle database. The driver model determines the necessary wheel torque request for the speed trace. This wheel torque request is then input into the running controller model. In parallel, GPS location information from the drive cycle database and current vehicle speed are input into the local speed prediction algorithm, which outputs the vehicle speed prediction. This vehicle speed prediction serves as an input, along with the current ESS SOC, to the predictive powertrain controller. The predictive powertrain controller determines the optimal engine power as a function of time between the present and the end of the prediction horizon. This optimal engine power is the second external input into the running controller model (along with the wheel torque request). This running controller model enforces constraints on the powertrain so that the optimal powertrain requests cannot violate powertrain torque, speed, and SOC constraints. The running controller model feeds requests for the engine, motor and generator torques and speeds to the plant model, which simulates the physical components in the vehicle. The relevant outputs from the vehicle plant model are fuel consumed, ESS SOC and vehicle speed.

This FE model makes it possible to evaluate the tradeoffs of different prediction horizons. If the prediction horizon is very short, accurate speed predictions can be made. However, the predictive powertrain controller can only realize a limited FE benefit due to the short prediction

horizon. Conversely, with longer prediction horizons, the predictive powertrain controller can find more optimal ways to operate the engine to minimize the fuel consumed over the prediction horizon. However, with longer prediction horizons, the speed predictions will be less accurate and the predictive powertrain controller will be optimizing for speeds that the vehicle may not actually travel.

Simulations of different prediction horizons are developed to explore these tradeoffs. Simulations for prediction horizons of 5, 10, 15, 20, 30, 45, 60, 90, and 120 seconds are developed. In addition, idealized cases are explored. Simulations where the speed prediction algorithm is removed and instead the actual speed trace is used as an input to the predictive powertrain controller are developed for the same array of prediction horizons. These represent cases in which perfect speed predictions could be made. The information flow for this scenario is represented in Figure 7.

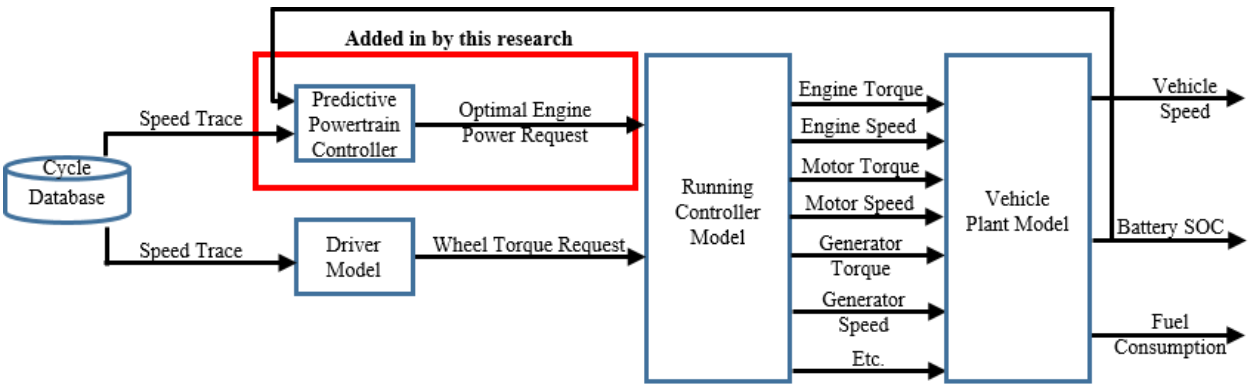

Figure 7: Information flow through the FE model, including perfect prediction and predictive powertrain controller

Under this perfect prediction scenario, the predictive powertrain controller with dynamic programming derives the powertrain control that results in the maximum possible FE for that prediction horizon. By comparing this to the FE of speed prediction simulations with real-world prediction, we can gain an understanding of the impact that real-world prediction errors have on

FE. Also, by comparing the FE results from speed prediction simulations to that of the baseline controller, we can quantify the degree to which FE benefit is robust to real-world prediction errors.

2.2 LOCAL PREDICTION RESULTS AND DISCUSSION

Before evaluating the FE benefit of different prediction horizons, a better understanding of the tradeoffs between prediction horizon and prediction fidelity needs to be obtained.

2.2.1 Tradeoffs between Prediction Horizon and Prediction Quality

Speed prediction error is calculated as the difference in the predicted and actual speed at each second of the prediction horizon. Then, the RMSE (Eq.1) for the prediction horizon is calculated. Within the vehicle simulations, the speed prediction algorithm is called at 1 Hz, so there is a RMSE calculation each second. Figure 8 shows the speed prediction RMSE distribution for each second of the drive cycle, and for different prediction horizons, along with the mean and bounds of one standard deviation of the prediction RMSE.

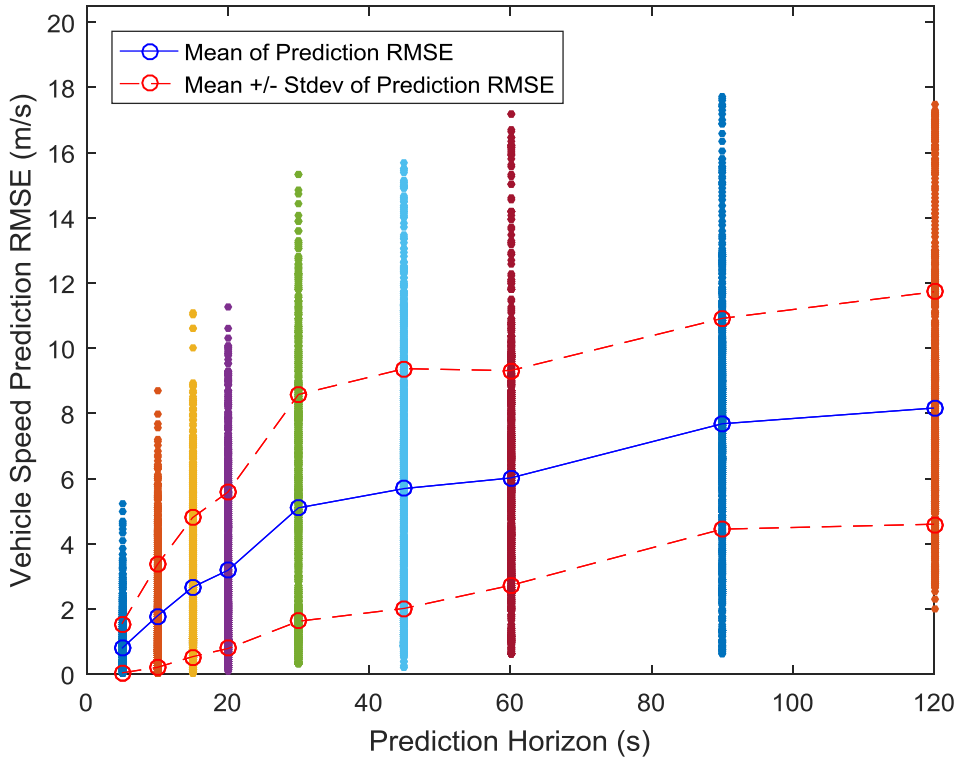

Figure 8: Scatter plot of prediction RMSE as a function of prediction horizon, along with the mean and bounds of one standard deviation of the prediction RMSE for each prediction horizon

As hypothesized in the research questions discussion, a shorter prediction horizon results in speed predictions that are more accurate. Conversely, longer prediction horizons result in larger speed prediction errors. As the prediction horizon grows, the prediction error becomes larger. For the larger prediction horizons, the prediction error reaches a saturation point because there is an inherent limit that is reached. For example, if the vehicle speed in the training dataset never eclipses 30 m/s, 80 m/s will not be predicted.

Figure 9 (a) illustrates the shape of these speed prediction RMSE distributions for a shorter prediction horizon (5 seconds in this sample result). The prediction RMSEs are more concentrated, with many near zero error. As the prediction horizon increases, the RMSE become less concentrated, with a larger standard deviation. However, the standard deviation of prediction RMSE also reaches a saturation point, as is illustrated in Figure 9 (b) and (c). It can be seen that

for 45 and 120-second prediction horizons, the standard deviations of RMSE are comparable; however, the mean of prediction RMSE increases as prediction horizon increases.

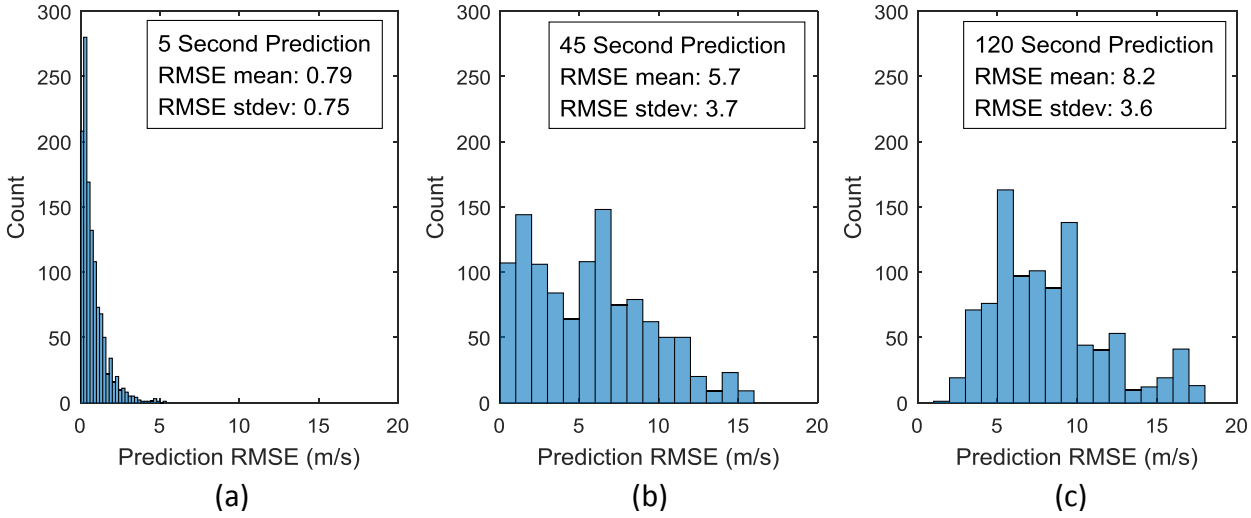

Figure 9: histograms of RMSE to compare how the magnitude of prediction RMSE increases as prediction horizon increases, but standard deviation reaches a saturation point

While predictions that are more accurate are desirable, there is a drawback to shorter prediction horizons, as they result in less information being supplied to the predictive powertrain controller. Thus, while shorter prediction horizons provide predictions that are more accurate, they are inherently limited in the FE gain that can be achieved. If a prediction horizon is too short, there will not be enough information available to realize a FE benefit over the baseline controller. If the prediction horizon is too large and there is too much prediction error, the predictive powertrain controller will be optimizing for incorrect speed predictions and again, no FE benefit may be realized. It is also possible that this prediction can result in a FE decrease over the baseline. This could occur if the prediction horizon is so short that the optimization routine is too limited by the SOC constraint that it cannot find FE benefit. In addition, a decrease in FE could occur if the speed predictions are so erroneous that optimal engine power vastly differs from what is needed to power the vehicle. However, these are extreme cases, and only might happen at very short or very long

prediction horizons. A moderate range of predication horizons is explored to find the prediction horizon that yields the largest FE improvement.

2.2.2 Engine Operation Comparison between Optimal and Baseline Control

A brief discussion of how the predictive powertrain controller derives FE improvement is included in this section. A comparison of engine power between the baseline and a 20-second prediction horizon simulation is shown in Figure 10. Note this is a subset of the drive cycle, as the cycle is over 20 minutes long.

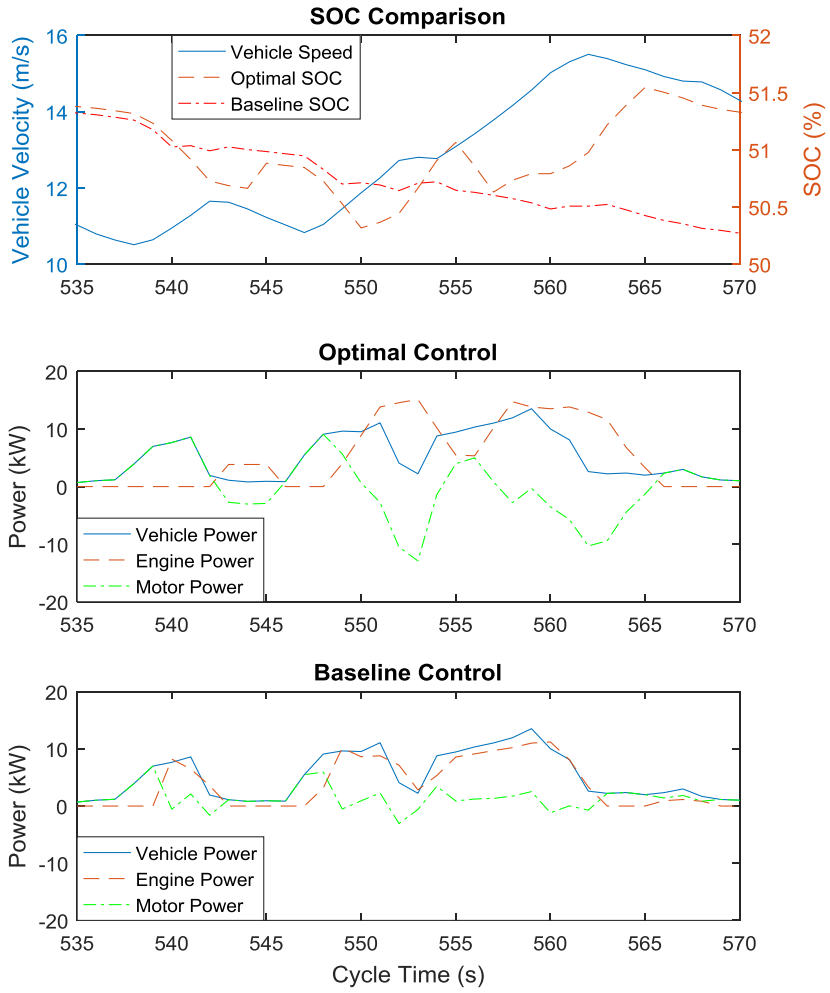

Figure 10: A sample baseline and speed prediction engine power comparison, along with SOC and speed trace over the segment with a prediction horizon of 20 seconds.

The predictive powertrain controller leverages the knowledge of future speeds to realize FE benefit by keeping the engine off as much as possible, which is illustrated in Figure 10 between 535-545 seconds. When the engine is turned on, it does so when more power is needed and operates along the ideal operating line (IOL). High efficiencies are achieved at higher engine loading. The result is that the engine tends to run at a higher power than the baseline when it is operating, displayed between 550-565 seconds in Figure 10. For further explanation of how the dynamic programming algorithm in the predictive powertrain controller realizes FE improvements, refer to previous studies completed at CSU [32], [53].

2.2.3 FE Benefit of Different Prediction Horizons for Cycles 1-3

With the implementation of the speed prediction and predictive powertrain controller and a better understanding of the tradeoffs between prediction horizon and prediction error, we now seek to develop a simulation-based quantification of the FE benefit as a function of prediction horizon. Simulations of the custom drive cycles using the rules-based baseline controller were developed for a baseline comparison. Additionally, simulations of the custom drive cycle using the predictive powertrain controller with perfect speed "predictions" (the actual speed trace) were developed for each prediction horizon. This serves as a best-case scenario representing the FE benefit that could be realized from this predictive powertrain controller if perfect predictions could be achieved.

Then, simulations are developed for each prediction horizon using speed prediction as the input to the predictive powertrain controller. As described in section 2.1.5, a NARX NN, trained for each specific prediction horizon, outputs speed predictions that the predictive powertrain controller uses as inputs to develop the optimal engine control for that speed prediction. This routine is repeated at 1 Hz in simulation time, while the model is driving the drive cycle.

Three drive cycles were investigated in this study. One drive cycle was recorded during relatively low traffic, mid-morning on a weekday in Fort Collins, CO (referred to as cycle 1). The other two were recorded at times with high traffic in Fort Collins, CO, during the evening weekday rush hour (referred to as cycles 2 and 3). All three cycles were during normal weather conditions, as all of the training data was also recorded during normal weather conditions. Investigating the effects of adverse weather is out of the scope of this study.

To evaluate the FE benefit from each simulation, the fuel consumed during the simulated drive cycle, along with the ending ESS SOC and distance traveled, are extracted from each simulation. The SAEJ1711 Jun. 2010 Recommended Practice for Measuring the Exhaust

Emissions and Fuel Economy of Hybrid-Electric Vehicles, Including Plug-in Hybrid Vehicles is used to calculate the charge-sustaining miles per gallon equivalent (CS MPGe) fuel economy.

Due to the stochastic nature of NN training, each time the NARX NN is trained, it will produce a slightly different set of weights and biases, causing it to output a different output for the same input. Additionally, with a short drive cycle such as this, variations in the ending SOC have a noticeable effect on CS MPGe. To account for this, each prediction horizon FE result is presented as a stochastic result, including n=5 trained NARX NNs, driven over each drive cycle. Figure 11 - Figure 13 are box plots that present this variation. These illustrate both the stochastic nature of NARX NN as well as the overall trend of how the prediction horizon length affects the FE benefit.

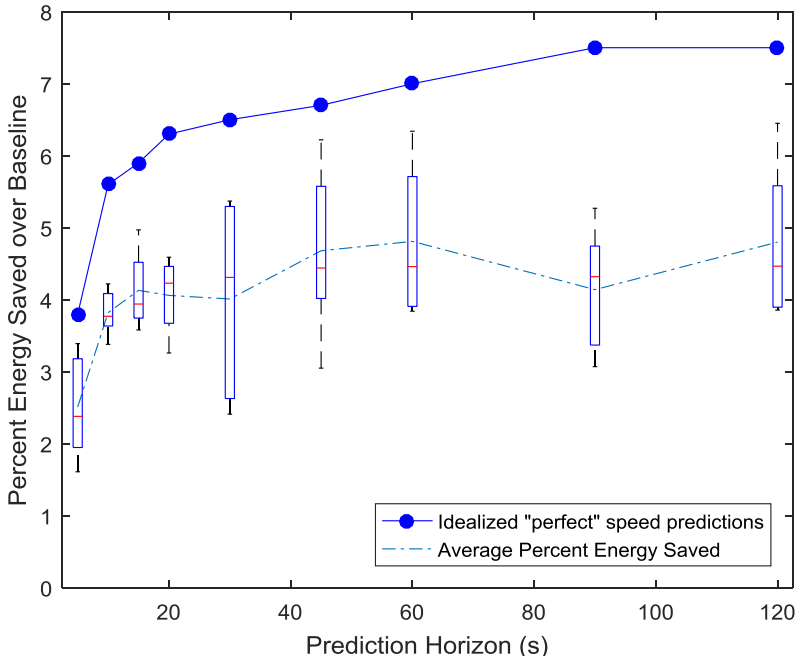

Figure 11: Box plot of percent energy saved by the local prediction method over the baseline controller, and comparison to perfect prediction simulations for Cycle 1.

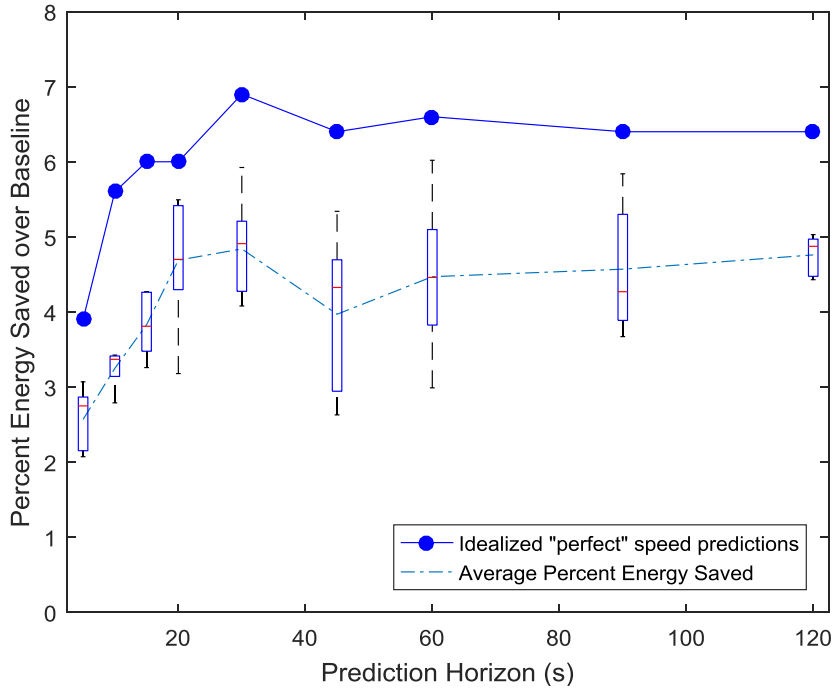

Figure 12: Box plot of percent energy saved by the local prediction method over the baseline controller, and comparison to perfect prediction simulations for Cycle 2.

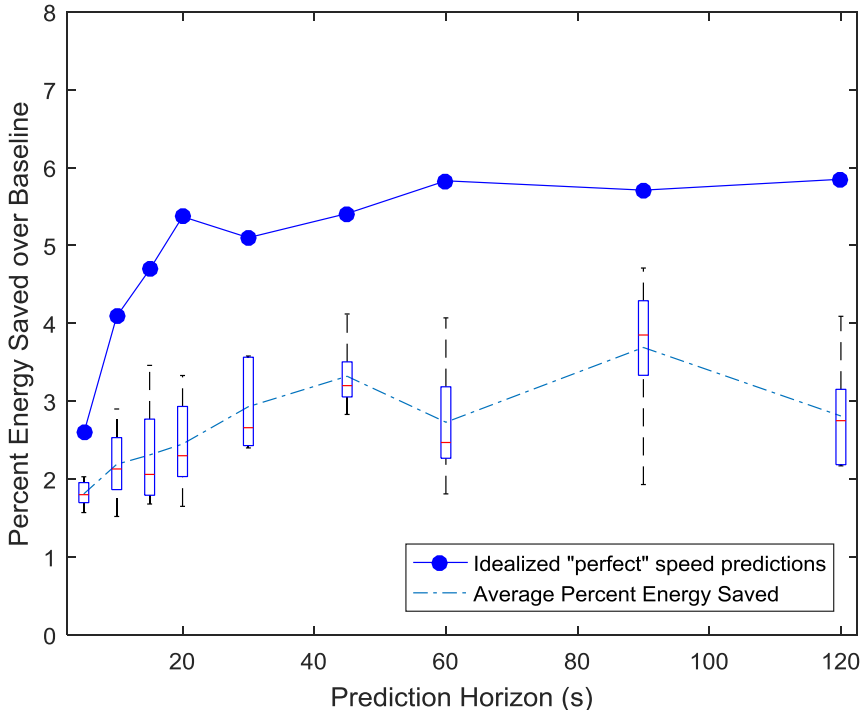

Figure 13: Box plot of percent energy saved by the local prediction method over the baseline controller, and comparison to perfect prediction simulations for Cycle 3.

The average CS MPGe, percent energy saved over the baseline, and percent of perfect prediction FE achieved for each of the prediction horizons and drive cycles is shown in Table 2. It can be seen that up to 4.8% CS MPGe improvement over the baseline can be achieved with long prediction horizons. This was calculated using the percent change equation,

$$\%\ change = \frac{FE_{prediction} - FE_{baseline}}{FE_{baseline}} \tag{4}$$

where $FE_{prediction}$ is the CS MPGe of the velocity prediction simulation and $FE_{baseline}$ is the CS MPGe of the baseline simulation. Additionally, up to around 75% of the potential FE benefit that could be derived with perfect prediction can be achieved by the proposed speed prediction method.

Table 2: Results of local data based predictions in terms of CS MPGe, the average percent energy saved over the baseline of 5 NARX NN trainings and the percent of the perfect prediction gains that was achieved via this prediction.

	Cycle 1			Cycle 2			Cycle 3		
prediction horizon (s)	CS MPGe	Avg % energy saved over baseline	% of perfect prediction	CS MPGe	Avg % energy saved over baseline	% of perfect prediction	CS MPGe	Avg % energy saved over baseline	% of perfect prediction
baseline	58.9	0%	0%	58.4	0%	0%	57.6	0%	0%
5	60.4	2.5%	65%	59.9	2.6%	67%	58.7	1.8%	70%
10	61.2	3.8%	68%	60.3	3.3%	58%	58.9	2.2	53%
15	61.4	4.1%	70%	60.6	3.8%	63%	59.0	2.3%	49%
20	61.3	4.1%	64%	61.1	4.7%	78%	59.0	2.4%	46%
30	61.3	4.0%	62%	61.2	4.8%	70%	59.3	2.9%	57%
45	61.7	4.7%	69%	60.7	4.0%	62%	59.5	3.3%	61%
60	61.8	4.8%	68%	61.0	4.5%	67%	59.2	2.7%	47%
90	61.4	4.1%	55%	61.1	4.6%	71%	59.7	3.7%	65%
120	61.7	4.8%	64%	61.2	4.8%	74%	59.2	2.8%	48%

It is difficult to discern overall trends from only three drive cycles where the results display as much variability as these do, but a couple generalizations can be made. First, as expected, shorter prediction horizons are not as beneficial as longer prediction horizons. However, the longer horizons have more speed prediction error associated with them, which can hinder the FE benefit. This increased chance of significant prediction error causes there to be non-smooth trends as the

prediction horizons increase. Additionally, as the prediction horizon increases, there are more issues with the predictive powertrain controller's ability to charge-sustain, as longer predictions are more erroneous. One final, important, thing to note is all prediction horizons investigated resulted in FE improvement over the baseline. This suggests that this prediction method is robust to real-world prediction error, and that commercially available technology can be incrementally implemented to achieve improved FE.

There are instances where an increased prediction horizon results in a worse FE for the perfect prediction (and, often, similarly for the prediction simulations as well). At the end of the drive cycle, prediction is stopped one prediction horizon length from the end of the cycle and the baseline controller is used for the rest of the cycle. Thus, predictions are ended at different times along the drive cycle. It was considered to end predictions at the same time for all prediction horizons, however prediction horizons up to 120 seconds were investigated and on an 8 mile drive cycle, that is a significant portion of the cycle so it would limit the amount of FE benefit shorter prediction horizons could achieve. Instead, the perfect prediction simulations are stopped at the same time as the corresponding speed predictions, so an even comparison is drawn.

It can be seen for this particular drive cycle that between 60 and 90 second prediction horizon results in the largest average FE benefit. These represent the best balance of prediction horizon and prediction accuracy for the prediction horizons explored. Prediction horizons shorter than this realize less FE benefit because less information being supplied to the predictive powertrain controller. Prediction horizons longer have a higher likelihood of predicting erroneously, which is shown by the larger maximum and minimum trends for the longer prediction horizons.

Since longer prediction horizons are more erroneous and the predictive powertrain controller optimizes engine control for the predicted speed, some simulations for longer prediction horizons

did not fully charge-sustain. The rules-based baseline controller has strict charge-sustaining behaviors and, thus, when the baseline controller was implemented for the end of the cycle; it quickly achieved a CS SOC, at the expense of fuel consumed. Simulations where this occurred resulted in lower FE than similar simulations that charge-sustained more effectively. This, combined with prediction error, causes sub-optimal engine control, which accounts for the difference in FE between the perfect prediction and local speed prediction simulations. A longer drive cycle would diminish the effect of the baseline controller achieving a charge-sustaining state, more effectively isolating the difference between perfect and speed predictions as solely caused by prediction error.

2.2.4 FE Benefit of Different Prediction Horizons for the Combined Cycle

In an attempt to reduce the sensitivity of FE to the ending SOC, simulations where all three cycles were concatenated together were developed. This cycle is referred to as the combined cycle. As with cycles 1-3, the combined cycle was simulated five times for each prediction horizon. Figure 14 shows the variance in each prediction horizon by incorporating box plots for percent energy saved over the baseline simulation. It can be seen that, in general, the box plots are smaller, indicating that SOC sensitivity is a large cause of variability of FE results in the shorter drive cycles and that the longer drive cycle reduced this sensitivity.

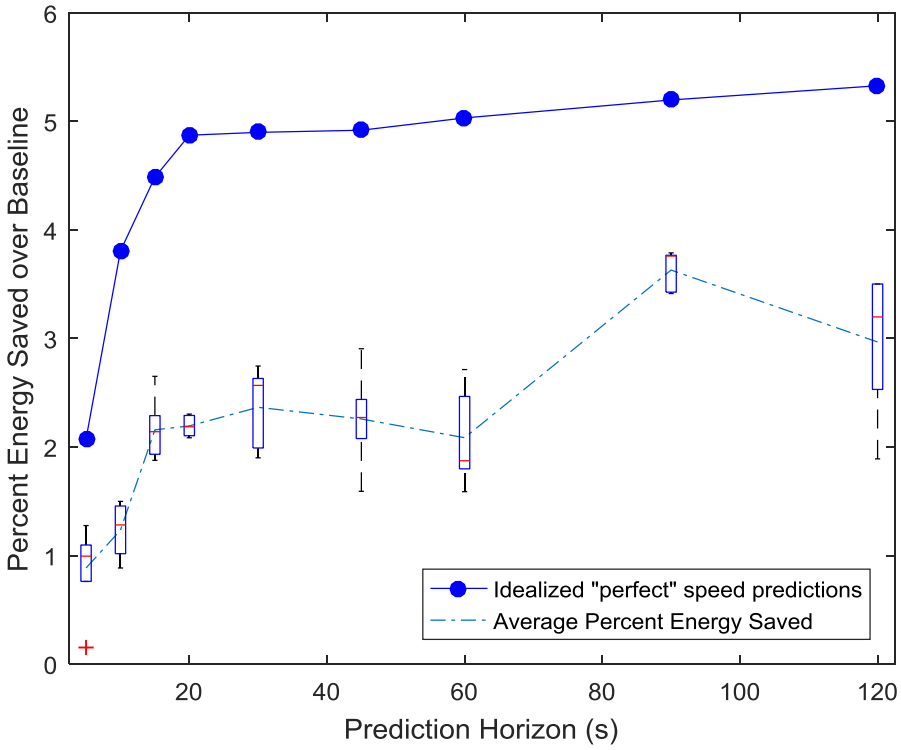

Figure 14: Box plot of percent energy saved over the baseline controller, and comparison to perfect prediction simulations for the combined cycle. The reduced size of the boxes shows that ending SOC has a significant impact on the variation between simulations of the same prediction horizon.

It should also be noted that the FE improvement for both speed prediction and perfect prediction simulations is reduced in comparison to the shorter cycles, as the baseline CS MPGe is higher for the combined cycle than it is for any of the other cycles. Further investigation into this, and more generally, the effect of drive cycle length on FE improvement should be explored. However, it is out of the scope of this study. Despite the reduced potential FE improvement, similar trends as cycles 1-3 are seen with the combined cycle.

2.3 Local Prediction Conclusions

This study shows that this method of real-world implementable speed prediction can yield FE improvements over the baseline for hybrid electric vehicles when coupled with a predictive powertrain controller. The results also show that a large portion – up to 75% – of the FE that could

be realized from perfect speed prediction can be achieved with this speed prediction from a NARX Neural Network trained with previous real-world driving data from the same route. This indicates that even with real-world prediction error, FE improvement can be realized.

This method can have a wide variety of applications. In this study, information about the entire drive cycle is used throughout the cycle. However, the application is not limited by that. If there is previous data recorded for a segment of the route, this prediction method could still be leveraged, thus information about the whole route is not necessarily needed. It should be noted that there are situations in which this method would not be fruitful. For example, if the SOC of the ESS were too low, the predictive powertrain controller would be limited in how the engine can be operated. Similarly, during highway driving situations, it is typically necessary to have the engine operating the majority of the time.

The results of this study suggest that for this type of mixed driving prediction horizons around 60-90 seconds provide the best potential for FE improvements in this vehicle. These represent the best tradeoff between gaining enough future information (prediction duration) and making speed predictions which are accurate enough to still consistently realize FE benefits (prediction fidelity). However, it is difficult to make generalized claims about how prediction duration and prediction fidelity will affect FE benefits from this study alone.

Additionally, technological advances, such as V2V or V2I communication, should increase the capability to predict accurate future speeds for larger prediction horizons. This methodology, which can be implemented using today's technology, could continue to provide more FE benefit as predicting capability increases.

3. SPEED PREDICTION METHOD 2: V2V COMMUNICATION

3.1 V2V PREDICTION METHODS

Prediction-based EMS aims to maximize fuel economy by predicting the vehicle speed for an upcoming segment of time and optimizing engine control for that prediction horizon, all in real time. This prediction method utilizes limited V2V communication and previously recorded driving data to predict future vehicle velocities. To investigate the tradeoff between prediction horizon and prediction error, a range of prediction horizons is evaluated for their effect on vehicle FE.

The goal of this study is to compare the vehicle FE for differing prediction horizons, to a baseline with no speed prediction, and to an idealized case with perfect speed prediction. These comparisons will allow for a better understanding of the impact of real-world prediction errors on potential FE benefits.

3.1.1 Baseline Vehicle Fuel Economy Model

The same rules-based baseline vehicle FE model that was described in Section 2.1.1 is utilized in this V2V communication speed prediction study.

3.1.2 Drive Cycle Development

The same drive cycle that was discussed in section 2.1.2 is used for this prediction method. We seek to capture the same mix of generic city and highway driving, in a compact drive cycle. Additionally, it is desired to compare the accuracy of these two different prediction methods, thus using the same drive cycle allows for such a comparison.

3.1.3 V2V Communication Simulation

In order to make vehicle speed predictions based on V2V communication using real-world data, a method of simulating V2V communication while obtaining driving data is necessary. To simulate this, the drive cycle was driven with two vehicles closely following each other. The vehicle in front will be considered the "lead vehicle" and the second vehicle will be considered the "ego vehicle." Speed predictions will be made for the ego vehicle. Each was equipped with data logging equipment; vehicle speed and GPS location information was recorded for both. From these two sets of recorded data, a common GPS location was used to set an adjusted start time and from this, the spatial and temporal relationship of these two datasets is extracted. Figure 15 is an overlay of the two velocity traces for one of the drive cycles investigated after the start time adjustment.

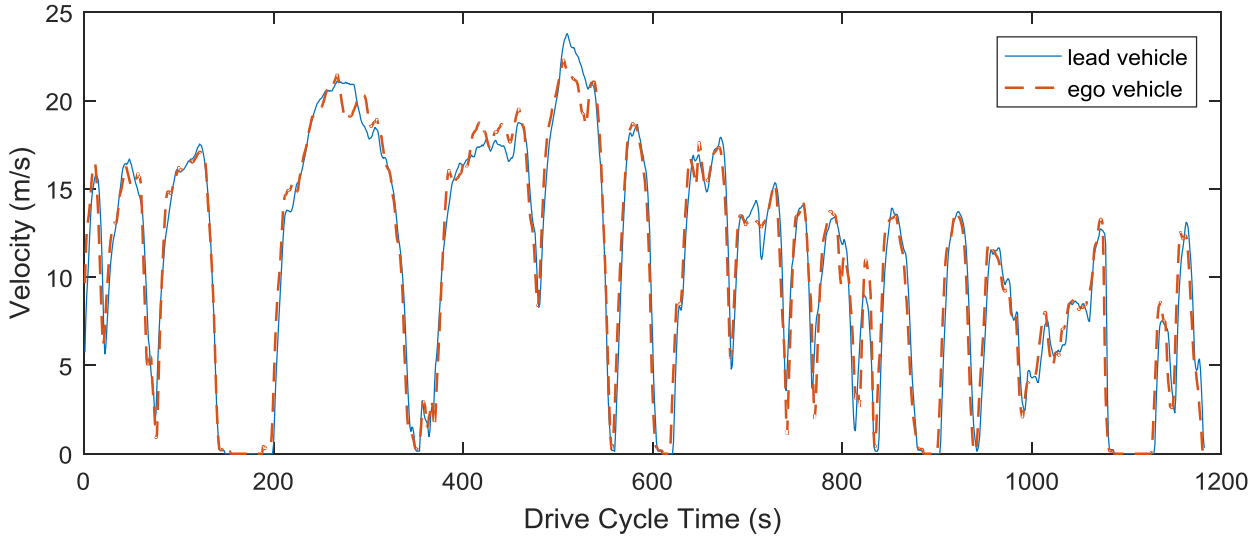

Figure 15: Ego and lead vehicle speed trace overlay with time synchronization for simulated V2V communication

The adjusted speed traces are used to simulate V2V communication between the two vehicles. In this study, we assume the lead vehicle communicates its vehicle velocity and GPS location information to the ego vehicle. This experimental setup allows for different amounts of information exchange to be explored. However, this was not in the scope of this study. It is

assumed the ego vehicle obtains information from the lead vehicle that is 5 seconds in the future from the ego vehicle's current state.

Discussion on the assumption of being able to obtain information from a vehicle that is 5 seconds ahead is as follows. Digital Short Range Communication (DSRC) is accepted as the form of initial V2V communication. Some model-year 2017 vehicles are equipped with DSRC in America [56] and Toyota already released some vehicles in Japan with DSRC capabilities [57]. The National Highway Traffic Safety Administration (NHTSA) has proposed a mandate that all light duty vehicles have V2V capability by 2019, with all new vehicles having it by 2023. Information that is proposed to be broadcasted are things such as location, speed, braking, etc. [58]. Thus, this study aims to simulate DSRC-type communication. DSRC has a range of 200-300m. Under the assumption that vehicles will be traveling at a maximum speed of 35 m/s (~75 mph), and that 200m is a reliable range for DSRC, then even when traveling at this maximum speed, a vehicle 200m away will be about 5.8 seconds away. Thus, vehicles more than 5 seconds ahead of the ego vehicle will be able to communicate with it through DSRC.

There are other assumptions that are important to note about this method of simulating V2V communication. The study of simulating and investigating the impacts of communication errors (poor signal, invalid data, etc.) is out of the scope of this study, so it is assumed the information communicated is accurate. Additionally, this study assumes that there is always a vehicle broadcasting its velocity and location 5 seconds ahead of the ego vehicle.

3.1.4 V2V Vehicle Velocity Predictions

The ego vehicle utilizes the obtained information to make vehicle speed predictions. Many researchers have investigated making speed predictions based on V2V communication alone, but this research combines limited information communicated via V2V with previously recorded

driving data. The general process of this speed prediction method is to obtain future information from the lead vehicle, use this velocity and location information to identify which previous driving route is most similar to the current driving route, and, finally, use the most similar route to predict future vehicle velocities. This method can predict further ahead than the 5 seconds of information obtained from the lead vehicle. However, again, this relies on the assumption that the route has been driven before by the ego vehicle.

A two-layer feedforward NN is used to classify which drive cycle from the database of previously recorded drive cycles is most similar to the one that is currently being driven. The inputs to this NN are the lead vehicle's broadcasted velocity, longitude and latitude information. The output is which drive cycle from the database of cycles is most similar to the inputs. Figure 16 depicts the structure of the pattern recognition NN used in this research.

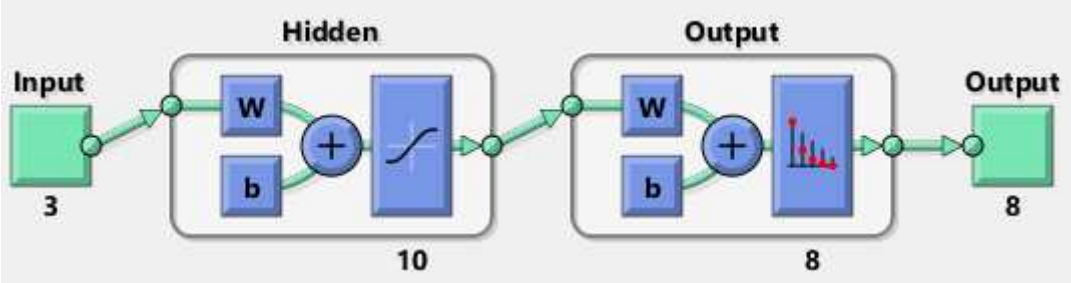

Figure 16: Structure of pattern recognition NN used to classify most similar drive cycle from lead vehicle information [55]

Data from eight recorded drive cycles are used to train, test and validate the pattern recognition NN. The pattern recognition NN has one hidden layer and is trained using scaled conjugate gradient backpropagation. This training method uses backpropagation to calculate the derivatives of the performance function with respect to weights and biases. These derivatives are used to update the weights and biases of the NN. Refer to Moller's article in *Neural Networks* journal for a more in-depth description of this training method [59]. Performance of the pattern

recognition NN is calculated by the cross-entropy method. This is used over a more general error calculation such as mean square error because it has a high penalty for extremely inaccurate outputs and low penalties for close to correct outputs [55]. This behavior is standard with pattern recognition algorithms.

The number of neurons in the hidden layer affects how well the NN can model the desired behavior. To determine the optimal number of neurons for this application, a range of different numbers of neurons in the hidden layer from 2 to 30 were explored. For each, a new NN is created and trained via the method described above. Since the NN's training process stochastic in nature, each time a NN is trained it will result in slightly different weights and biases, thus potentially affecting performance. To account for this, 10 NNs with the same number of neurons in the hidden layer were trained and the performance was averaged. However, there was essentially no cross-entropy performance difference between 5 and 20 neurons in the hidden layer from the training routine. Thus, we elected to evaluate 5, 10 and 20 hidden layer neurons further, for their effect on speed prediction errors.

As described above, the output of the NN is simply the drive cycle from the database that is the most similar to the information obtained from the lead vehicle. This drive cycle is referred to as the most similar cycle and is used to make velocity predictions. To make a velocity prediction, the location information from the lead vehicle is related to the corresponding location of the most similar cycle. From this, the most similar cycle is used to predict velocity for the prediction horizon.

3.1.5 Refinement of V2V Vehicle Velocity Predictions

There were multiple refinements made to the original velocity prediction method. The first refinement was to incorporate a "low speed shutoff" for the prediction. The need for this was

driven by the fact that since the speed prediction was merely the most similar drive cycle, there were times when the ego vehicle stopped in locations that were not captured in the drive cycle database (i.e. stoplights). This caused the speed prediction to be non-zero when the ego vehicle was stationary; an example of this behavior is shown in Figure 17. To correct for this, once the lead vehicle reached a minimum threshold velocity, the speed prediction was changed to be zero until the lead vehicle accelerated past the velocity threshold. It can be seen in Figure 16 that this "low speed shutoff" corrected for the erroneous prediction in this instance.

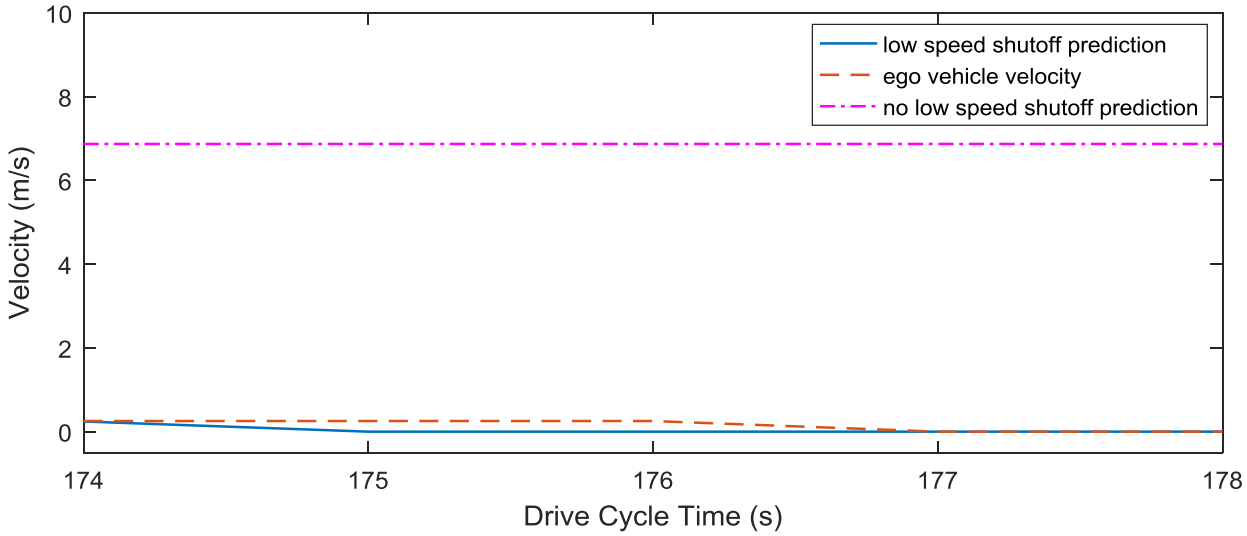

Figure 17: Example of low speed shutoff making better prediction when most similar drive trace did not come to complete stop.

The second refinement incorporated velocity information from the lead vehicle as the first 5 seconds of the prediction and then used the velocity trace from the most similar cycle over subsequent portion of the prediction horizon. This is desirable because it incorporates information from the lead vehicle as part of the prediction. However, this can lead to a discontinuity in the velocity prediction when switching from the lead vehicle information to the most similar cycle information. To correct for this discontinuity, an offset to the most similar cycle portion is applied. This offset is calculated by taking the difference between the last lead vehicle velocity point and

the corresponding velocity from the most similar cycle. This shifts the most similar cycle portion of the prediction to the lead vehicle velocity while still allowing for the same trend (acceleration/deceleration) from the most similar cycle to remain. Instances where this offset could be helpful could be during bad weather or traffic causing the flow of traffic to be generally lower, or an occasion where traffic is lighter than usual so the flow of traffic is higher. Examples of predictions where this method greatly reduced error in the prediction are displayed in Figure 18 (a-c). Additionally, if the most similar cycle was already a good predictor, this offset does not affect it, as shown in Figure 18 (d). It is ensured that prediction of negative velocities does not occur as a result of this offset. The third refinement, as mentioned in section 3.1.4, was to choose the number of hidden neurons that produced the lowest velocity prediction RMSE mean and variance.

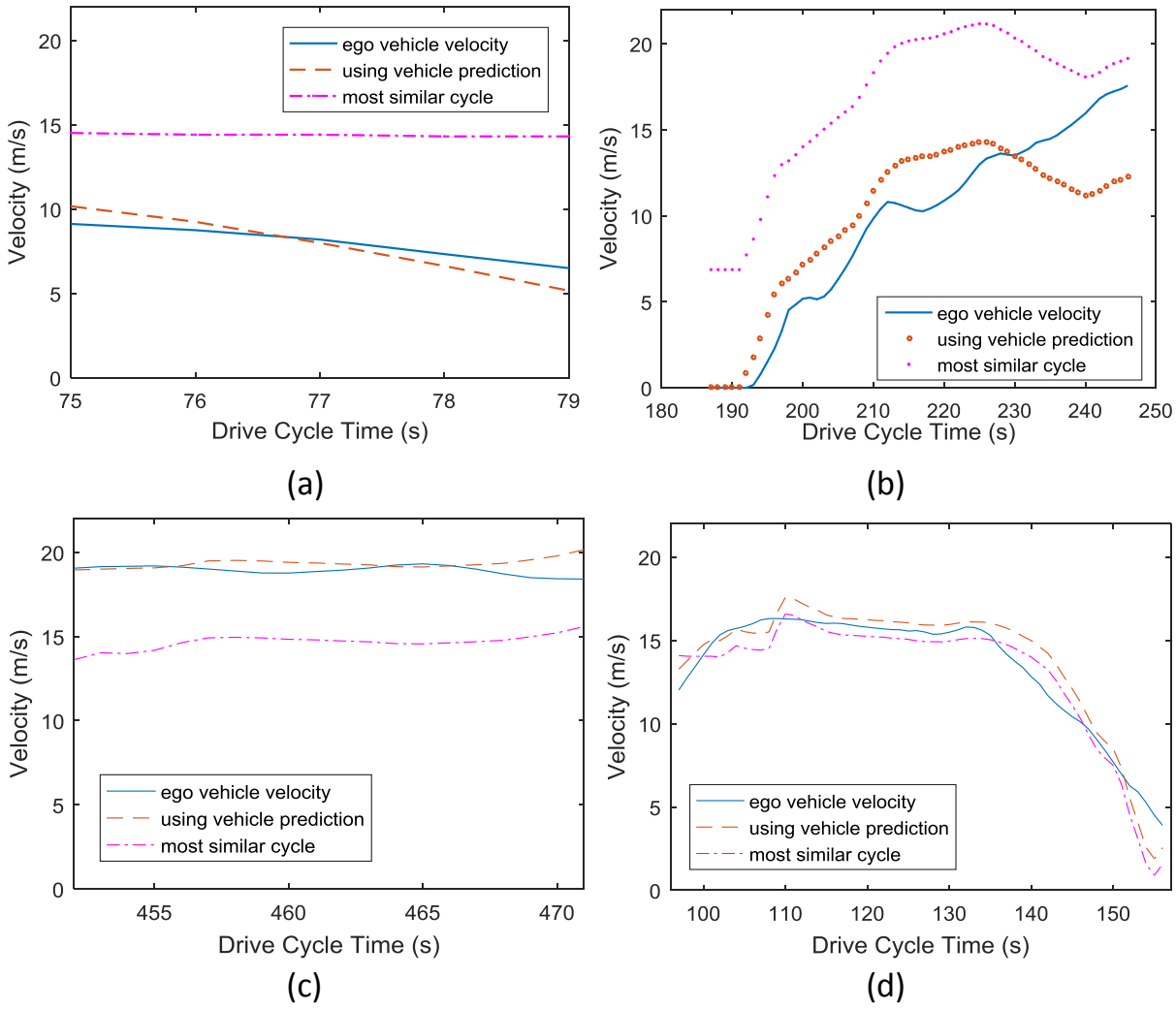

Figure 18: Examples of where incorporating V2V information and offset into prediction improves prediction fidelity. For (a), (b) and (c) the offset shifts prediction close to actual speed trace. In (d) the offset does not significantly affect prediction when most similar cycle is not erroneous.

To evaluate the effectiveness of these refinements, a design of experiments (DOE) was developed. For each of the three drive cycles investigated, every combination of the low speed shutoff on/off, incorporating lead vehicle information as prediction on/off, and the three number of neurons in the hidden layer of the pattern recognition NN were investigated. For each combination, a velocity prediction was produced at each second along the drive cycle and the RMSE was calculated for the prediction horizon. Thus, there was a RMSE produced every second. The mean and variance of the RMSEs over the entire drive cycle was calculated as the metrics of

accuracy for this DOE. Since training methods of NNs are stochastic, this entire process was completed 3 times for each number of neurons in the hidden layer (5, 10, and 20). It was observed that incorporating the lead vehicle velocity with the offset to the most similar cycle was superior to using only the most similar cycle. This held true for all number of neurons, and whether the low speed shutoff was on or off. Examples of this improvement on velocity predictions is shown in Figure 18 and on error statistics is shown in Figure 19, which shows the variance of the RMSE over all the prediction horizons for one drive cycle with 10 neurons in the hidden layer and the low speed shutoff not used.

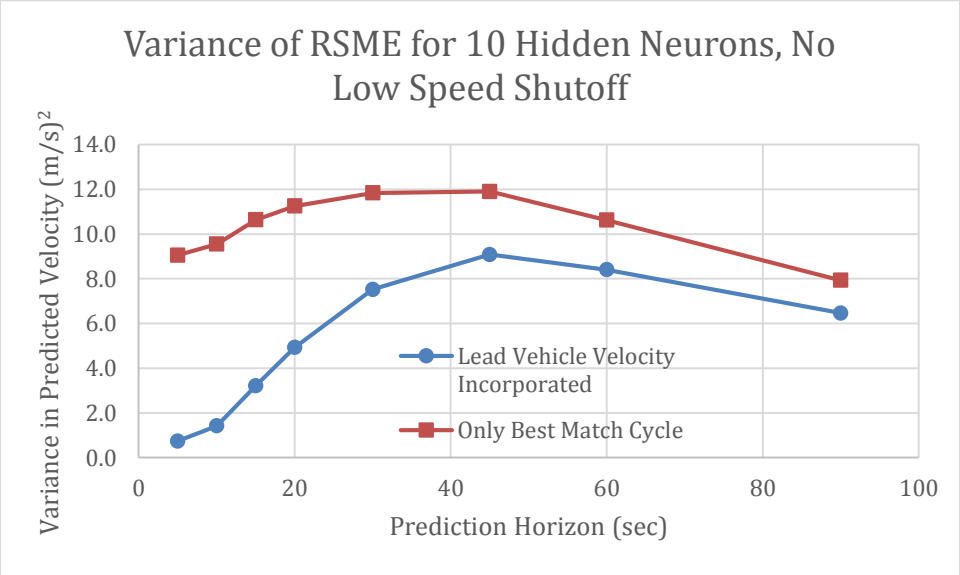

Figure 19: RMSE variance for 2 cases: only using the most similar cycle, and incorporating lead vehicle velocity information and offset into the prediction

The results of this DOE demonstrate that predictions without the low speed shutoff were more accurate. Two driving factors cause this. First, predicting velocities of zero for the long prediction horizons is not realistic, as it is not often that a vehicle remains idle for up to 90 seconds (one of the longer prediction horizons). Second, the velocity offset when transitioning from the lead vehicle velocity prediction to the most similar cycle, corrects for the instances when the lead

(and hence ego) vehicle is stopping but the most similar cycle does not stop. This offset still allows the acceleration phase to be predicted, resulting in predictions that are more accurate, as shown in Figure 20.

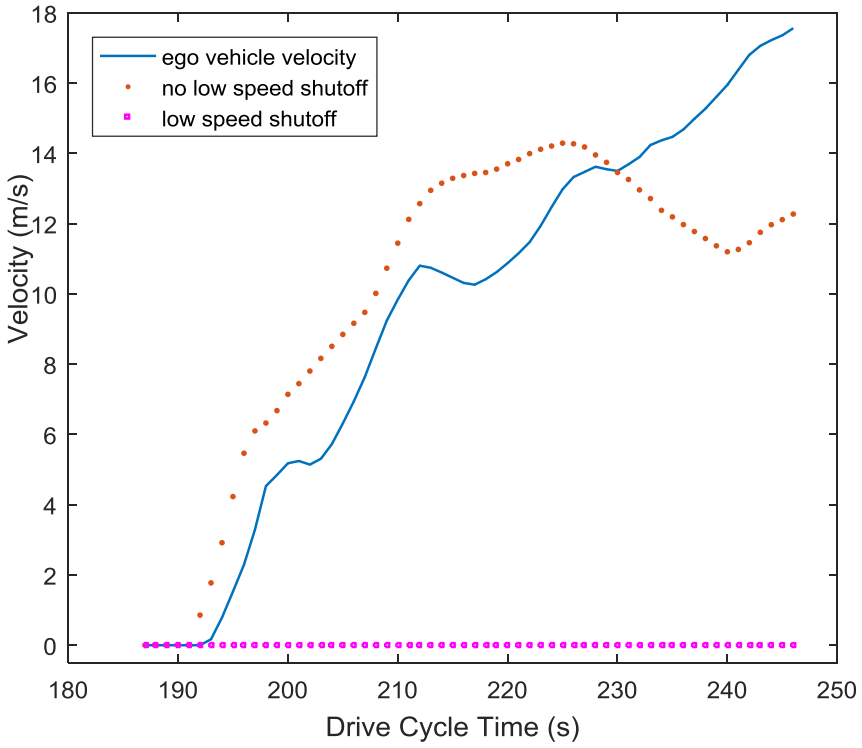

Figure 20: Example of low speed shutoff weakness, and lead vehicle prediction offset strength

Additionally, it was observed that the number of hidden neurons had a smaller impact on prediction accuracy than the other two factors investigated in the DOE. The differences between 5 and 10 neurons in the hidden layer were not discernable, and 10 neurons in the hidden layer was chosen.

3.1.6 Tradeoffs between Prediction Horizon and Prediction Quality

As logic suggests, with a shorter prediction horizon, predictions that are more accurate can be achieved. Conversely, longer prediction horizons result in predictions that are more erroneous. To investigate this, a range of prediction horizons is explored. The range of prediction horizons

are 5, 10, 15, 20, 30, 45, 60, 90, 120, 150 and 180 seconds. For this study, velocity prediction error is calculated by the RMSE for each prediction. Figure 21 shows the velocity prediction RMSE distribution for different prediction horizon lengths.

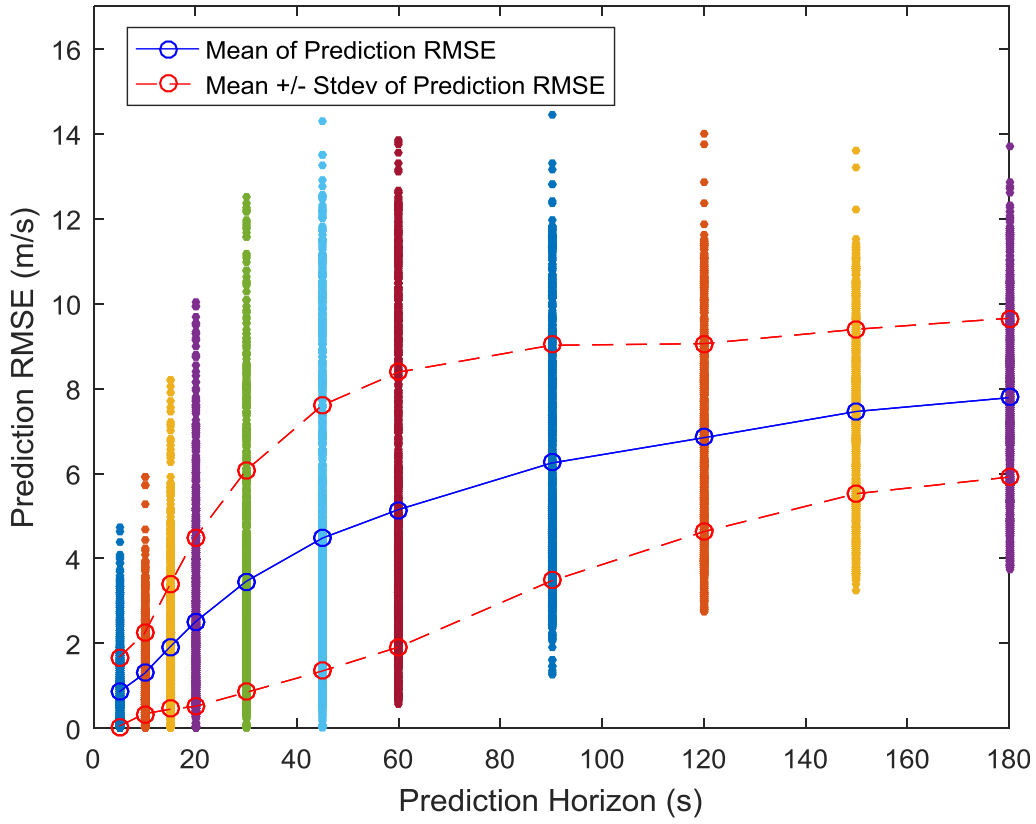

Figure 21: Scatter plot of prediction RMSE as a function of prediction horizon, along with the mean and bounds of one standard deviation of the prediction RMSE for each prediction horizon

As the prediction horizon grows, the prediction error does as well. However, the prediction RMSE reaches a saturation point because there is an inherent limit to how erroneous a velocity prediction will be. For example, if the vehicle speed in the training dataset never eclipses 30 m/s, 80 m/s will not be predicted. Similarly, the error is not likely to be 20 m/s for the entire prediction horizon (which would result in an RMSE of 20).

The standard deviation of prediction RMSE also reaches a saturation point. This can be seen in Figure 21 but is better exemplified in Figure 22. There reaches a point, around 45-60 second

horizon, where the standard deviation reaches a maximum, and then begins to decrease slightly as the prediction horizon continues to increase. This is because the predictions are becoming more erroneous, as seen in Figure 22, where for 180-second prediction horizon (c), the RMSE is centralized around 8 m/s, whereas for 5 seconds (a), it is clustered at 0 m/s, and for 45s (b), it is more varied.

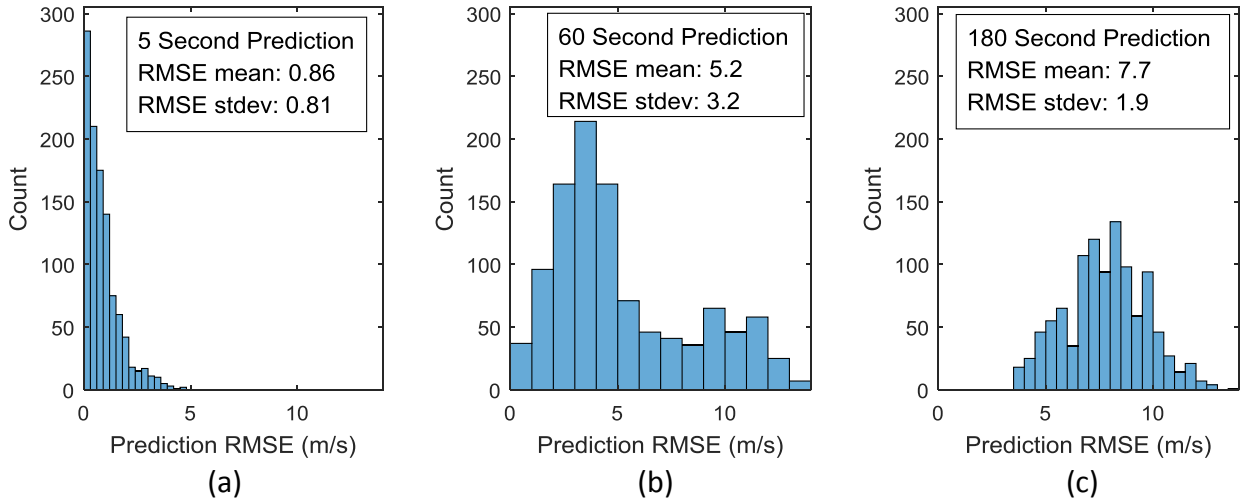

Figure 22: histograms of RMSE to compare how the magnitude of prediction RMSE increases as prediction horizon increases, but deviation reaches a saturation point, and actually decreases

These results demonstrate that if the prediction horizon is very short, accurate speed predictions can be made. However, the predictive powertrain controller can realize only a limited FE improvement for short prediction horizons. Conversely, with longer prediction horizons, the predictive powertrain controller can find more optimal ways to operate the engine over the prediction horizon. However, with longer prediction horizons, the speed predictions will be less accurate and the predictive powertrain controller will be optimizing for speeds that the vehicle may not actually travel. Further discussion of this tradeoff is in section 3.2.1.

3.1.7 Development of Predictive Powertrain Controller

The same predictive powertrain controller as described in section 2.1.4 is used. The only difference is that now the velocity inputs are coming from the V2V prediction algorithm, instead of the local prediction algorithm.

3.1.8 Implementation of Prediction and Predictive Powertrain Controller into FE Model

The only change to the FE model is that now the V2V prediction algorithm is used to make velocity predictions. Both prediction methods use GPS location as one of the inputs to the prediction algorithm. However, the V2V prediction algorithm contains velocity inputs from the lead vehicle. These changes are reflected in Figure 23. As with the local prediction method (section 2.1.5), the routine of making velocity predictions for the prediction horizon, and optimizing engine power for that prediction is repeated at 1 Hz.

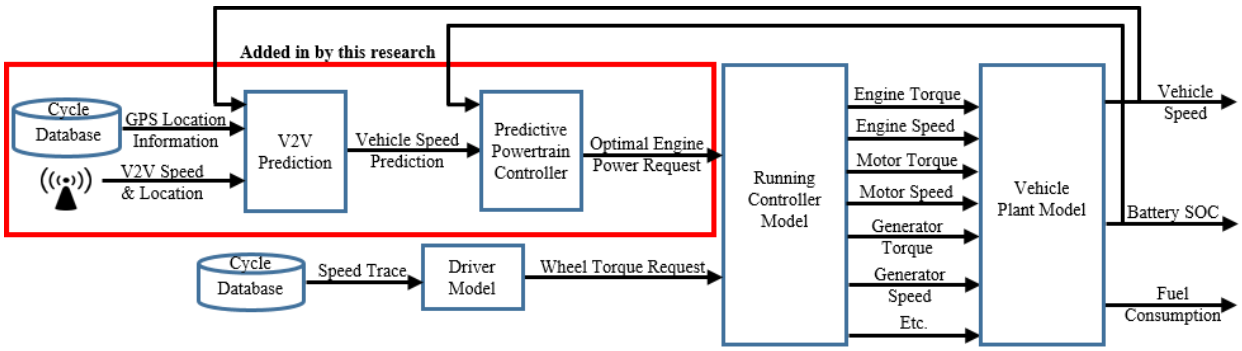

Figure 23: Information flow through FE model, including the V2V prediction method and predictive powertrain controller

Simulations of different prediction horizons are developed to explore the tradeoffs discussed in section 3.1.6. In addition, idealized cases are explored, as described in section 2.1.5. Under this perfect prediction scenario, the predictive powertrain controller with dynamic programming derives the powertrain control that results in the maximum possible FE for that prediction horizon. By comparing this to the FE of speed prediction simulations with real-world prediction, we can

gain an understanding of the impact real-world prediction errors have on FE. Also, by comparing the FE results from speed prediction simulations to those of the baseline controller, we can quantify the degree to which FE benefit is robust to real-world prediction errors.

3.2 V2V Prediction Results and Discussion

We seek to develop a simulation-based quantification of the fuel economy benefit as a function of prediction horizon. This will provide insight into the tradeoff between increasing prediction horizons and prediction fidelity. As the prediction horizon grows, more information is obtained for the predictive powertrain controller, but the predictions are more erroneous. This tradeoff can only be understood via a systems level analysis by incorporating the predictive powertrain controller and FE model.

3.2.1 FE Benefit of Different Prediction Horizons for Cycles 1-3

Three drive cycles were investigated in this study. One drive cycle was recorded during relatively low traffic, mid-morning on a weekday in Fort Collins, CO (referred to as cycle 1). The other two were recorded at times with high traffic in Fort Collins, CO, during the evening weekday rush hour (referred to as cycles 2 and 3). All three cycles were during normal weather conditions, as all of the training data was also recorded during normal weather conditions. Investigating the effects of adverse weather is out of the scope of this study.

Simulations for each prediction horizon are developed and compared to the baseline simulation, as well as the idealized case where perfect predictions over the same prediction horizon are possible. These comparisons provide two insights: first, the comparison to the baseline controller provides insight into whether or not this prediction method and predictive powertrain controller are robust to real-world prediction errors. Second, by comparing to the idealized case

we seek to understand how effective current and near-term technologies are in making vehicle velocity predictions.

After each simulation, the final ESS SOC, fuel consumed and distance traveled are extracted. The SAEJ1711 Jun. 2010 Recommended Practice for Measuring the Exhaust Emissions and Fuel Economy of Hybrid-Electric Vehicles, Including Plug-in Hybrid Vehicles is used to calculate the CS MPGe. Since NN training is stochastic, each prediction horizon is simulated five times to capture the variation that is incorporated with training differences. Additionally, with a short drive cycle such as this, variations in the ending SOC have a noticeable effect on CS MPGe. By running multiple simulations, these effects of variances can be explored.

Figure 24 - Figure 26 capture the variance in each prediction horizon by incorporating box plots for percent energy increased over the baseline simulation. These also show the perfect prediction scenario as well. This represents a ceiling for the percent energy that could be saved over the baseline controller for this drive cycle. Note that there are instances where an increased prediction horizon results in a worse FE for the perfect prediction (and, often, similarly for the V2V prediction simulations as well). At the end of the drive cycle, prediction is stopped one prediction horizon length from the end of the cycle and the baseline controller is used for the rest of the cycle. Thus, predictions are ended at different times along the drive cycle. We considered ending predictions at the same time for all prediction horizons, however prediction horizons up to 180 seconds were investigated and on an 8 mile drive cycle. The 180-second prediction window is a significant portion of the cycle and it would limit the amount of FE benefit shorter prediction horizons could achieve. Instead, the perfect prediction simulations are stopped at the same time as the corresponding V2V predictions, so that an even comparison is drawn.

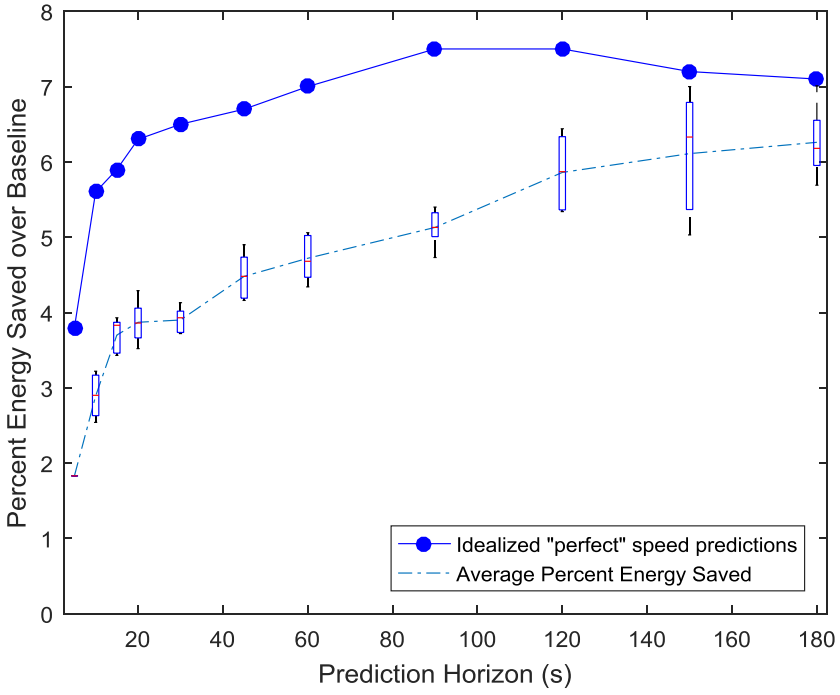

Figure 24: Box plot of percent energy saved over the baseline controller, and comparison to perfect prediction simulations for Cycle 1.

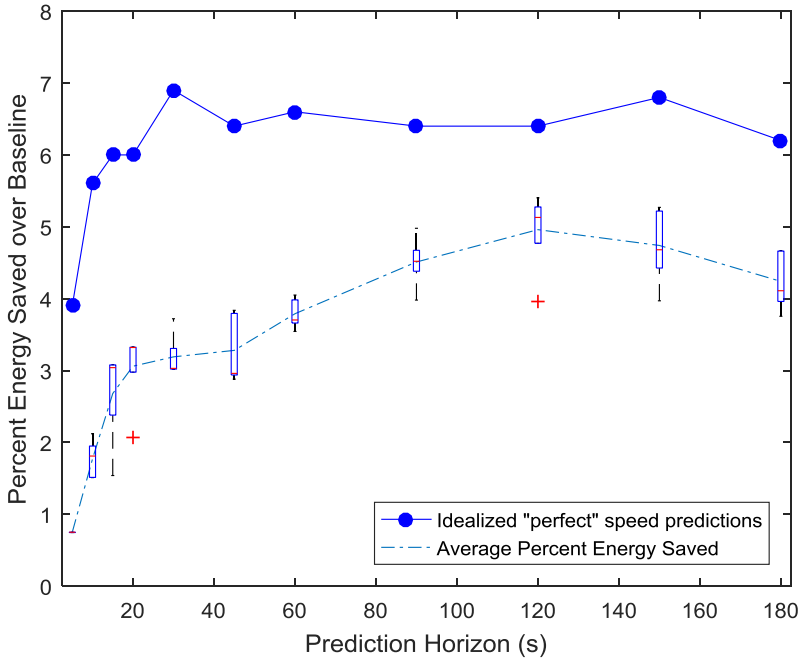

Figure 25: Box plot of percent energy saved over the baseline controller, and comparison to perfect prediction simulations for Cycle 2.

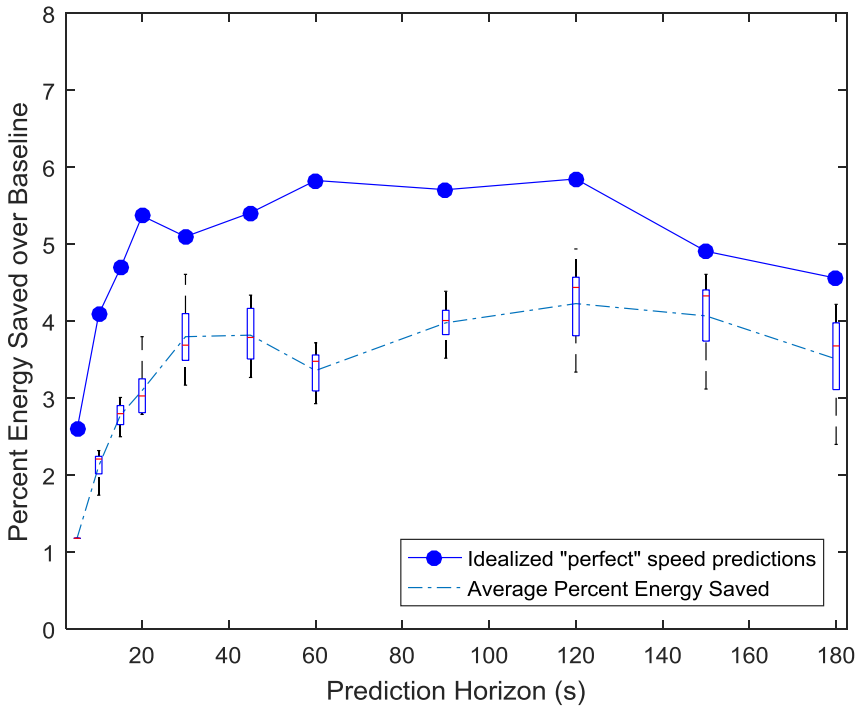

Figure 26: Box plot of percent energy saved over the baseline controller, and comparison to perfect prediction simulations for Cycle 3.

The average CS MPGe and average percent of energy saved over the baseline controller for all prediction horizons and individual drive cycles investigated is displayed in Table 3. Up to about 6% CS MPGe improvement over the baseline is achieved and up to about 85% of the potential FE benefit that could be derived with perfect prediction can be achieved by this speed prediction method. Additionally, few trends can be extracted from this study. First, only utilizing information from the lead vehicle (the 5-second prediction horizon) does result in increased FE, but only marginally. Only incorporating that information is not fruitful, a prediction method is also necessary to achieve significant FE improvements. Second, as the prediction horizon increases, so does the FE benefit. The point where FE benefit begins to decrease for long prediction horizons are where the benefit from gaining more future information is offset by the prediction being too erroneous. This tipping point was seen to be at 120-second prediction horizon for cycle 2 and 3. For cycle 1, the FE continued to increase for each prediction horizons investigated. There are a

few possibilities for this. Recall that cycle 1 was the cycle that was driven in non-rush hour traffic, whereas cycles 2 and 3 were in driven in rush hour traffic. Also, recall that the prediction method is completed by identifying the most similar cycle from a database of previously recorded drive cycles. If the database contains more cycles that are more similar to lower traffic periods, that could cause cycle 1 to increase FE more in comparison to cycles 2 and 3. It should be noted that longer prediction horizons were not investigated in this study because the drive cycle is eight miles long and takes ~20 minutes to drive. Thus, predicting more than three minutes ahead causes a significant portion of the cycle at the end to be driven on the baseline controller. Additionally, as the prediction horizon increases, there are more issues with the predictive powertrain controller's ability to charge-sustain, as longer predictions are more erroneous. One final, important, thing to note is all prediction horizons investigated resulted in FE improvement over the baseline. This suggests that this prediction method is robust to real-world prediction error, and that near-term technology can be incrementally implemented to achieve improved FE.

Table 3: Results of V2V communication based predictions in terms of CS MPGe, the percent energy saved over the baseline and the percent of the perfect prediction gains that was achieved via this prediction.

	Cycle 1			Cycle 2			Cycle 3		
prediction horizon (s)	CS MPGe	Avg % energy saved over baseline	% of perfect prediction	CS MPGe	Avg % energy saved over baseline	% of perfect prediction	CS MPGe	Avg % energy saved over baseline	% of perfect prediction
baseline	58.9	0%	0%	58.4	0%	0%	57.6	0%	0%
5	60.0	1.8%	48%	58.8	0.7%	19%	58.3	1.2%	46%
10	60.6	2.9%	52%	59.4	1.8%	31%	58.8	2.1%	52%
15	61.1	3.7%	63%	60.0	2.7%	44%	59.2	2.8%	59%
20	61.2	3.9%	61%	60.2	3.1%	51%	59.4	3.1%	58%
30	61.2	3.9%	60%	60.3	3.2%	46%	59.8	3.8%	75%
45	61.6	4.5%	66%	60.3	3.3%	52%	59.8	3.8%	71%
60	61.7	4.7%	67%	60.6	3.8%	57%	59.6	3.4%	58%
90	61.9	5.1%	69%	61.0	4.5%	70%	59.9	4%	70%
120	62.4	5.9%	78%	61.3	5%	77%	60.1	4.2%	72%
150	62.5	6.1%	85%	61.2	4.7%	70%	60.0	4.1%	83%
180	62.6	6.3%	88%	60.9	4.2%	69%	59.6	3.5%	77%

3.2.2 FE Benefit of Different Prediction Horizons for the Combined Cycle

As described in section 2.2.4, the FE of these simulations is sensitive to the ending ESS SOC. Simulations where the predictive powertrain controller was not able to fully charge-sustain resulted in lower vehicle FE than similar simulations that did fully charge-sustain. In an attempt to reduce the sensitivity of FE to the ending SOC, simulations where all three cycles were concatenated together were developed. This cycle will be referred to as the combined cycle. As with cycles 1-3, the combined cycle was simulated five times for each prediction horizon.

Figure 27 shows the variance in each prediction horizon by incorporating box plots for percent energy saved over the baseline simulation. It can be seen that, in general, the box plots are smaller, indicating that SOC sensitivity is a large cause of variability of FE results in the shorter drive cycles and that the longer drive cycle reduced this sensitivity.

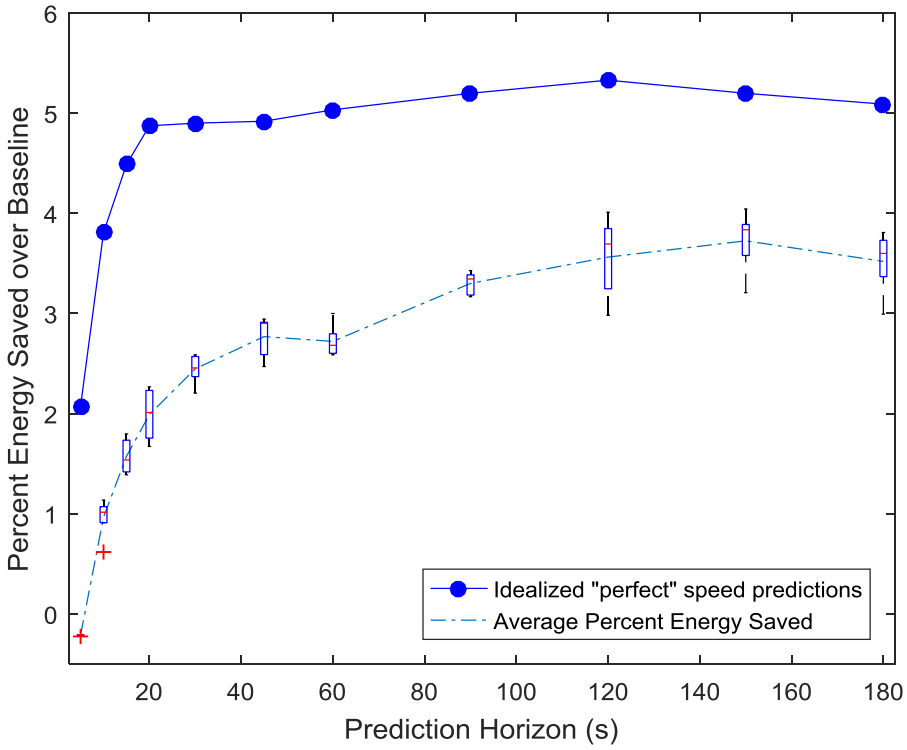

Figure 27: Box plot of percent energy saved over the baseline controller, and comparison to perfect prediction simulations for the combined cycle. The reduced size of the boxes shows that ending SOC has a significant impact on the variation between simulations of the same prediction horizon.

It should be noted that the FE improvement for both speed prediction and perfect prediction simulations is reduced in comparison to the shorter cycles, as the baseline CS MPGe is higher for the combined cycle than it is for any of the other cycles. The effect of drive cycle length on FE improvement should be investigated further. However, it is out of the scope of this study. Despite the reduced potential FE improvement, similar trends as cycles 1-3 are seen with the combined cycle.

3.3 V2V Prediction Conclusions

In this study, a vehicle velocity prediction method was developed that utilizes V2V communication involving only limited information exchange, along with previously recorded local vehicle information. The prediction method is trained and simulated using real-world data, so real-

world prediction errors are developed. This allowed the ability to see if velocity predictions are robust to real-world prediction errors. To evaluate how this prediction method can be employed to increase FE, a systems level analysis that incorporated the speed prediction method with a predictive powertrain controller and Toyota Prius HEV FE model was completed.

Different prediction horizons ranging from 5-180 seconds were investigated to understand the tradeoffs between increasing amount of information obtained at the expense of prediction fidelity. Short prediction horizons are limited by not obtaining as much information to be utilized by the predictive powertrain controller. However, long prediction horizons are more erroneous, causing the predictive powertrain controller to optimize for speed that the vehicle does not travel. Thus, there is a point where those opposing forces are equally offset. For this prediction method, on the drive cycles investigated, a prediction horizon of 120 seconds resulted in the greatest FE improvement.

Additionally, the results of these simulations show that FE benefits are robust to real-world prediction error, as all prediction horizons investigated resulted in FE improvements over the rules-based baseline controller. The V2V prediction simulations were also compared to an idealized case where perfect speed prediction was possible. This comparison allows us to understand the impact prediction error has on the potential FE improvement. For some of the longer prediction horizons, the V2V prediction simulations were able to achieve up to about 85% of the FE improvement of the perfect prediction simulations. As sensing technology improves, the gap between the speed prediction and perfect prediction scenarios will continue to decrease.

Overall, this study adds to the growing body of evidence that predictive powertrain control is more efficient the current reactive control. Additionally, it shows that predictions can be made

with technology that is on the brink of being commercially available on vehicles and that the predictions are robust to real-world prediction errors and drive cycle variability.

.

4. OVERALL RESULTS AND DISCUSSION

4.1 COMPARISON OF VELOCITY PREDICTION METHODS

Two methods of speed prediction were developed in this study; the first utilizes only local, previously recorded driving data to make future speed predictions. The second utilizes limited V2V communication information and incorporates that with local, previously recorded driving data to make future speed predictions. This section seeks to compare these two prediction methods via two methods of comparison. The first compares the prediction methods based on RMSE calculations. The second uses FE as the metric of prediction accuracy, which results in a more holistic view of prediction fidelity. Additionally, the first 5 seconds of both prediction methods is explored further to provide insight into differences between information obtained from other vehicles and local information.

4.1.1 Prediction Method Comparison

This section compares the prediction methods by investigating the RMSE in speed prediction for each prediction horizon of both prediction methods. Predictions are made every second along the drive cycle and the RMSE of the prediction is calculated for each prediction. The mean and variance of the RMSEs over the entire drive cycle are calculated for each prediction method. Figure 28 illustrates the trends of RMSE mean for five different iterations of both the local and V2V prediction methods of cycle 1. Figure 29 illustrates the prediction RMSE variance for five different iterations of both the local and V2V prediction methods. Figure 37- Figure 40 (in appendix 1) demonstrate the RMSE mean and variance for the other two cycles investigated. It can be seen that the V2V prediction method results in lower and more consistent mean and variance of prediction RMSE.

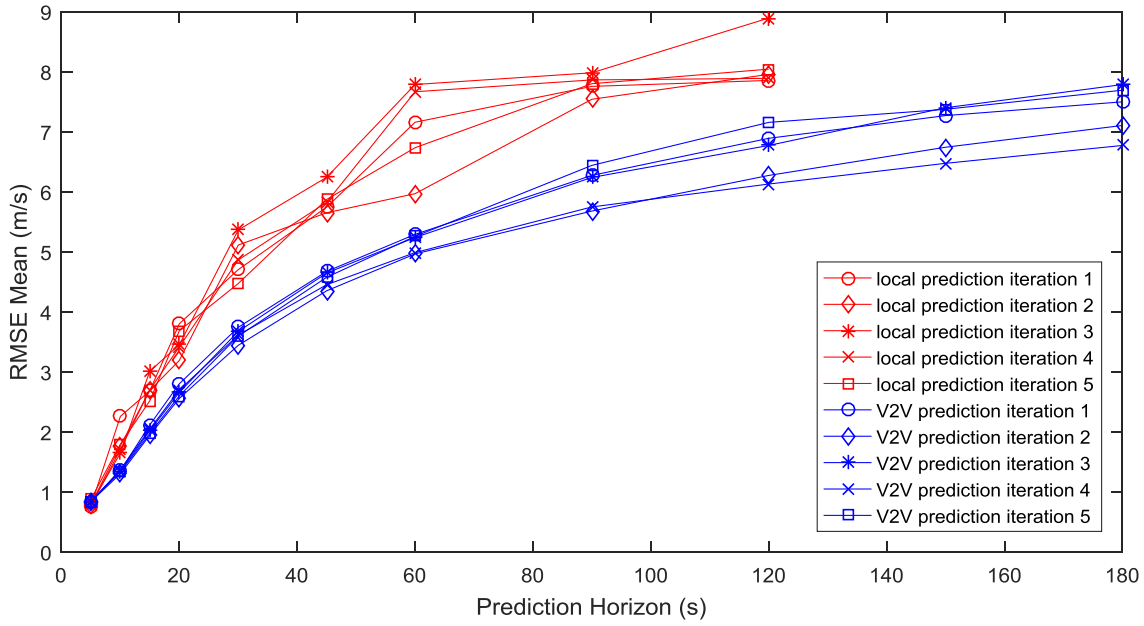

Figure 28: Comparison between local and V2V prediction methods via RMSE mean of all predictions from cycle 1

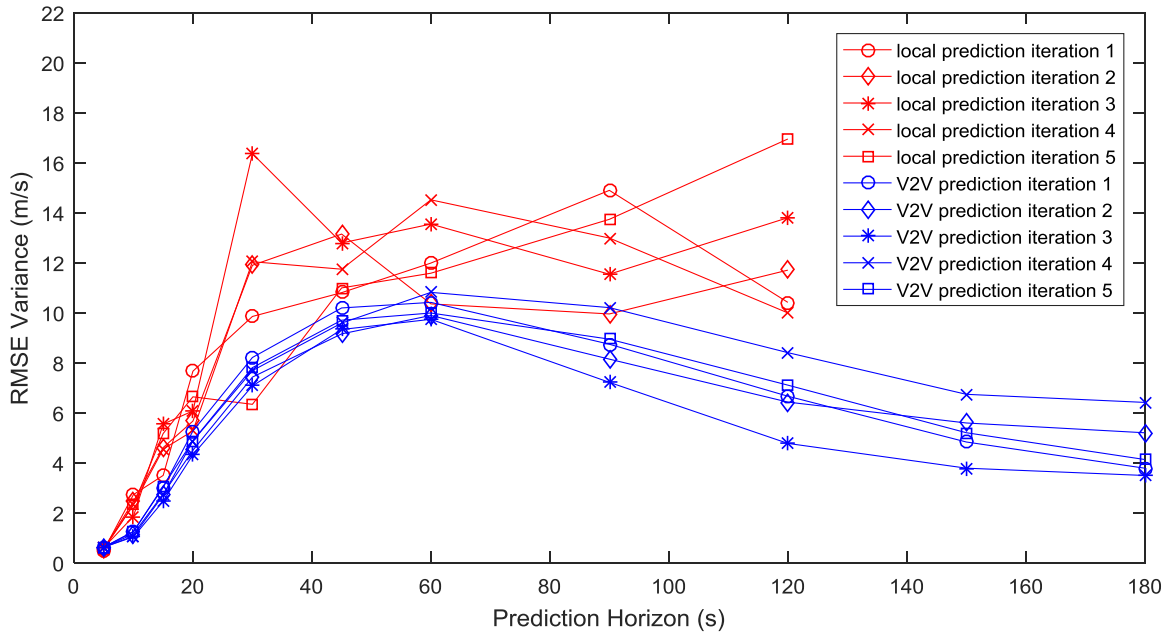

Figure 29: Comparison between local and V2V prediction methods via RMSE variance of all predictions from cycle 1

Improved velocity prediction RMSE is not necessarily indicative of an improvement in terms of FE, which is stakeholders' top priority. This is the case because during acceleration/decelerations, any shift in time for the prediction (even with similar trends), will result

in large calculated RMSE. Examples of predictions with a larger RMSE but that are actually perhaps beneficial for FE improvement because they trend with the actual velocity trace are shown in Figure 30. The corresponding RMSE calculations are included in Table 4.

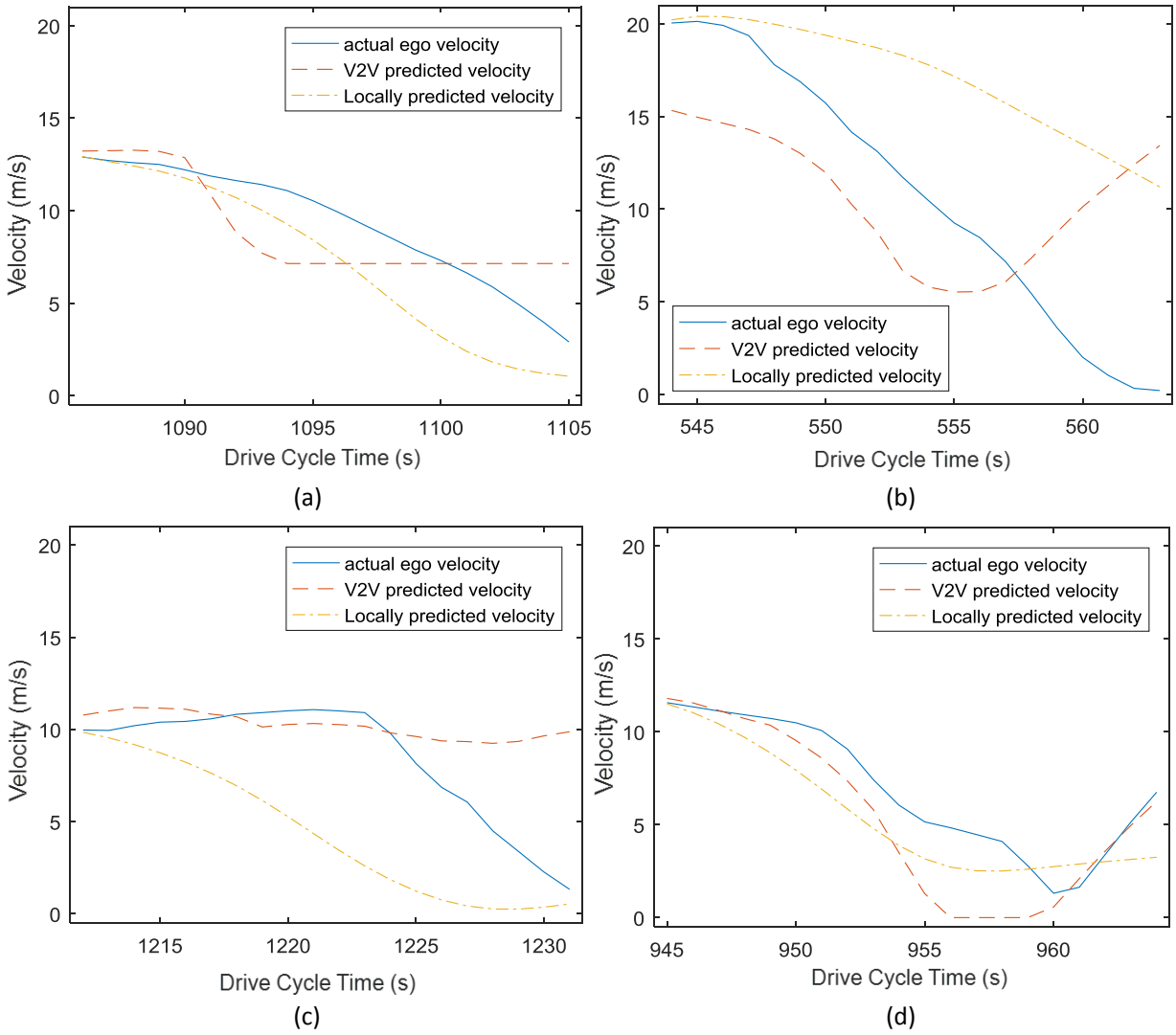

Figure 30: Illustrative examples of when lower RMSE quantification may lead to less accurate prediction of vehicle velocity

Table 4: Corresponding RMSE Calculations that show examples of RMSE calculations not providing accurate descriptions of prediction accuracy.

Corresponding Figure	V2V RMSE (m/s)	Local RMSE (m/s)
(a)	6.23	7.45
(b)	2.23	1.99
(c)	2.24	2.50
(d)	3.25	4.86

This type of comparison can be used to compare the prediction accuracy. However, this comparison does not provide insight into their "overall value" to the system level view of investigating FE. Thus, the prediction methods will be compared in terms of FE in the next section.

4.1.2 Fuel Economy Comparison

To gain a better understanding of the costs and benefits between these two prediction methods, a systems level analysis is completed. By evaluating the prediction methods through the metric of FE, we can determine which prediction method is superior. Figure 31 illustrates the average FE benefit over the baseline for each of the four cycles investigated. It can be seen that there is no significant difference in the overall performance of the three individual drive cycles, but the overall FE improvement potential for the combined cycle is lower. In general, the local prediction is more accurate at shorter prediction horizons, although, those do not gain as much FE as longer prediction horizons do. It should be noted that for the 5-second prediction horizon, the local prediction actually performed better than the V2V prediction. This indicates that the local prediction method produces more accurate predictions than the lead vehicle's velocity. This is discussed further in section 4.1.3.

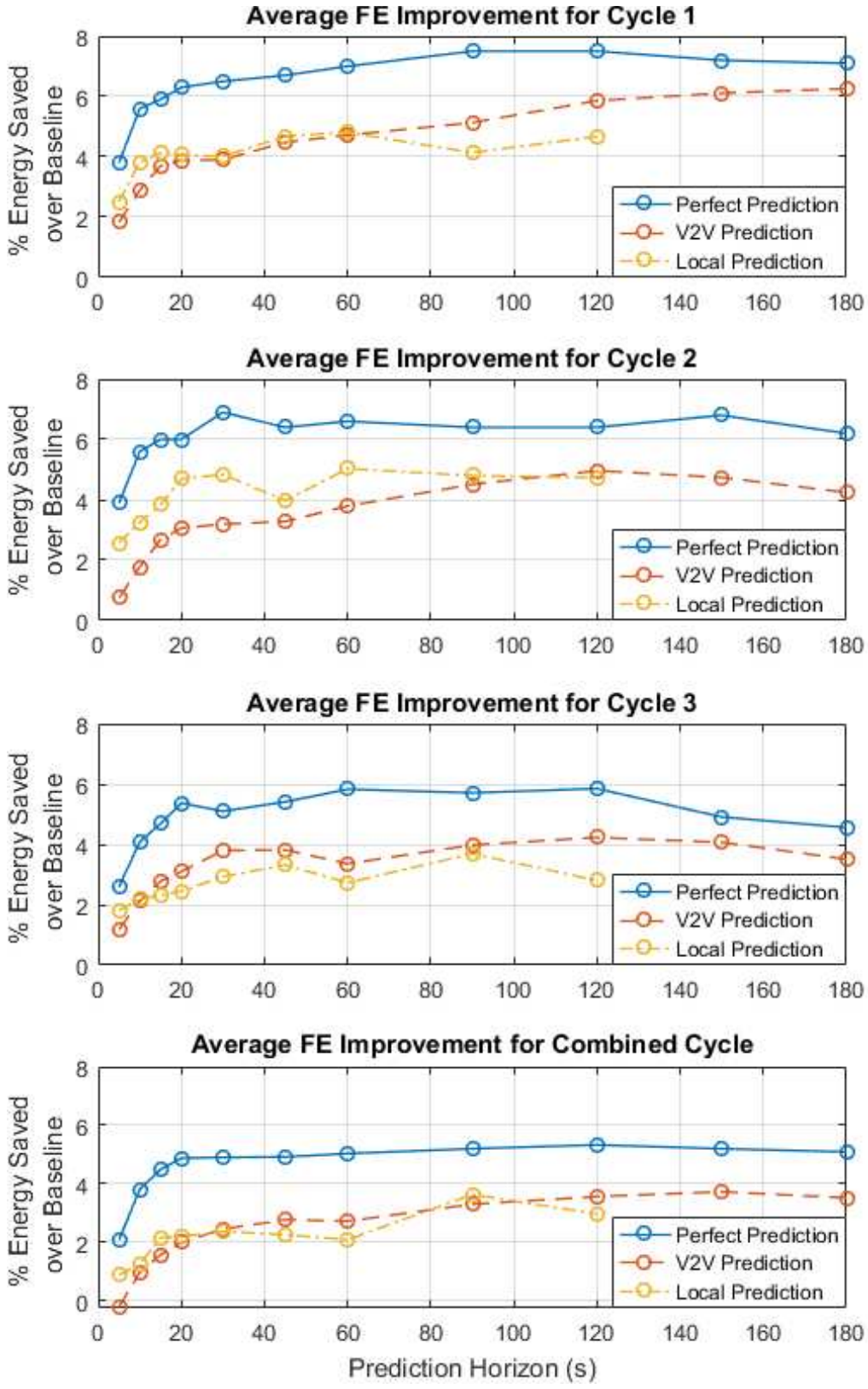

Figure 31: Comparison between local and V2V prediction methods of average FE improvement over baseline reactive EMS for all three drive cycles as well as the combined cycle

For longer prediction horizons, the V2V method consistently realized a higher FE improvement over baseline than the local prediction method. This indicates that choosing one drive cycle as the prediction is, overall, more accurate than the prediction produced by the NARX NN. The fact that the V2V prediction method improves FE more consistently for longer prediction horizons is consistent with the RMSE comparison of the two prediction methods. It should be noted that the local prediction method had issues with not achieving a charge-sustaining state. Additionally, for long prediction horizons (greater than 120 seconds) the local prediction would sometimes produce predictions that were so erroneous that the predictive powertrain controller could not find a solution. Thus, simulations greater than 120-second prediction horizons were not completed for the local prediction method.

While the local prediction method is limited in its prediction horizon, it is able to achieve significant improvements over the baseline controller, and only utilizes technology that is readily available on vehicles today. This suggests that prediction methods such as this can begin to be implemented into today's vehicles to switch from reactive to predictive energy management strategies. Looking into the near future, DSRC V2V communication is being implemented on some model-year 2017 vehicles, and will become commercially available in the next few years. The V2V prediction method proved to produce predictions that are more accurate for longer horizons, and is only utilizing information that will be communicated over initial V2V communication. This method also has the ability to utilize more information that might be shared between vehicles in the future, such as the lead vehicle broadcasting its own velocity prediction, which could be utilized to further improve both prediction accuracy and achievable prediction horizon lengths.

4.1.3 Comparison of 5-Second Prediction Horizon

Figure 31 illustrates that, in all 4 cases of the 5-second prediction horizon, the local prediction method realized a larger FE benefit than the V2V prediction method. This is particularly interesting because for the V2V prediction method, the 5-second prediction horizon is simply the V2V communicated information. This ascertains that the local prediction method for 5 seconds is actually more accurate than velocity information obtained from a vehicle traveling directly in front of the ego vehicle. We hypothesize that this could be a result of the local prediction method being trained on driving data from the ego vehicle, so the driver's driving characteristics (i.e. accelerations and braking aggressiveness) are learned by the local prediction method whereas in the V2V method, there is no relation between the drivers in the lead and ego vehicles. To test this hypothesis, a comparison of the predicted and actual vehicle accelerations for both prediction methods is completed. The average acceleration for each 5-second prediction and the corresponding 5 seconds of actual vehicle acceleration were plotted on x and y axes, respectively. This is illustrated in Figure 32 (a) for the local prediction method and Figure 32 (b) for the V2V prediction method for cycle 2.

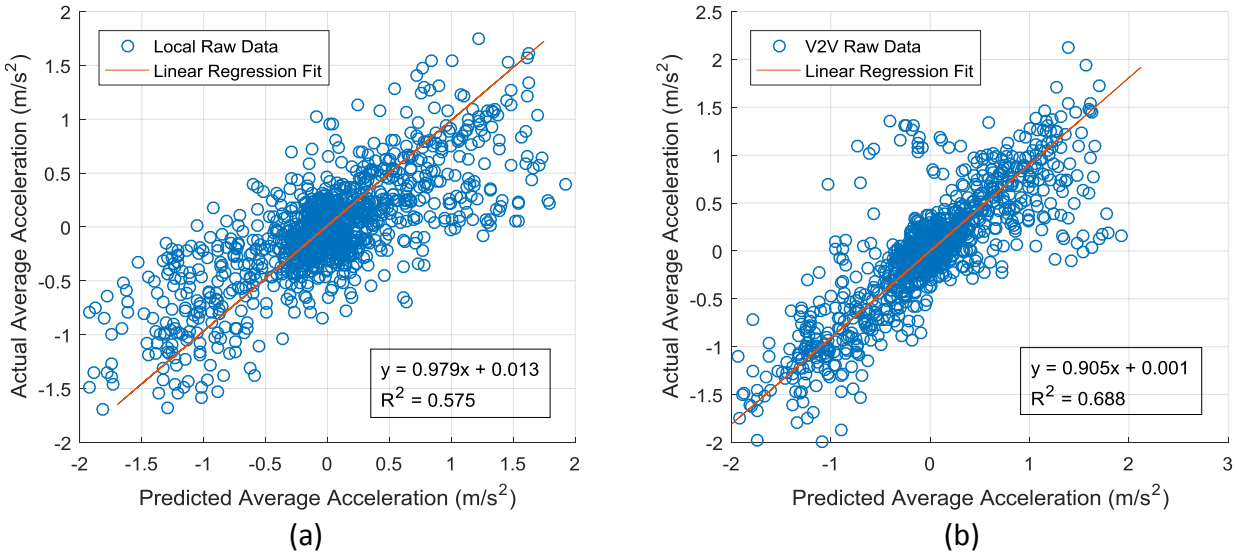

Figure 32: Comparison of predicted and actual vehicle accelerations with linear regression provides insight into why the local prediction method (a) realizes a larger FE benefit than the V2V prediction method (b) for 5-second prediction window on cycle 2

A linear regression of the raw data provides insight into the relationship between the actual and predicted vehicle accelerations. If the predictions were perfect, this plot would have a linear regression with a slope of 1, which would indicate that each of the predicted and actual velocities were the same. The closer the linear regression slope is to 1, the more similar the predicted acceleration is to the actual vehicle acceleration. Since the actual vehicle acceleration is plotted on the y-axis, linear regression slopes that are greater than 1 means the actual accelerations are larger (or more aggressive) than the predictions. Linear regression slopes less than 1 indicate that the predicted accelerations are more aggressive than the actual vehicle accelerations.

Figure 32 illustrates that the linear regression slope of the local prediction method is closer to 1 than the V2V prediction method – 0.979 compared to 0.905. Thus, the predicted accelerations derived from the local prediction method were closer to the actual vehicle accelerations than those of the V2V method, which supports our hypothesis. Similar trends can be seen for the other two individual cycles, illustrated in Figure 41 and Figure 42 in Appendix 0.

Note that the coefficient of determination (R^2) for the local prediction method is lower than that of the V2V prediction method, indicating that the V2V linear regression is a better fit. This indicates that, while the local prediction method produces predictions where the accelerations are more similar to the actual vehicle overall, there is more variation compared to the V2V prediction method. This can also be seen visually in Figure 32.

4.2 ESS CAPACITY LIMITATION

It can be seen in Figure 31 that the FE benefit over the baseline controller reaches a saturation point where larger prediction horizons do not realize larger FE benefit. This is caused by vehicle architecture limitations, specifically the capacity of the ESS. There is no added benefit to predicting further into the future than the amount of time it would take to charge/discharge the ESS. For example, even with more information, the predictive powertrain controller would not be able to save ESS power for a lot of stop and go behavior at the end of the drive cycle. Further evidence of this saturation can be seen in Table 5. This presents the FE benefit of the 4 cycles investigated for the perfect prediction scenario with a 120-second prediction horizon, as well as the FE benefit if the entire drive cycle could be predicted perfectly.

Table 5: Comparison of FE improvement of perfect prediction for 120-second prediction horizon and full cycle prediction

	Cycle 1	Cycle 2	Cycle 3	Combined
FE benefit 120s horizon	7.44%	6.41%	5.85%	5.33%
FE benefit entire cycle	7.50%	7.41%	6.87%	5.82%

It can be seen that there is not much more FE improvement over the baseline controller for predicting the entire (roughly 20 minutes for the shorter cycles) drive cycle, as there is with only

predicting 120 seconds ahead. Thus, if the ESS were larger, as is in a PHEV, this saturation limit would be pushed out to a longer prediction horizon. For example, the Prius simulated in this study has a 1.31 kWh ESS, whereas the first generation of the Prius PHEV (2012-2015) has a 4.4 kWh ESS. The saturation point of where the predictive powertrain controller is limited by the ESS capacity would be extended significantly if a PHEV were studied.

4.3 ENGINE OPERATION COMPARISON FOR DIFFERENT PREDICTION HORIZONS

We also desire to understand the impact of prediction horizon on the way the predictive powertrain controller operates the engine. To understand this, two different prediction horizons over the same cycle are investigated. This computational experiment seeks to understand whether different amounts of velocity prediction information have a significant impact on the optimal engine operation. In the figures below, the speed predictions are displayed, along with the drive cycle, SOC, engine power and fuel consumed for both the shorter (20-second) and longer (60-second) prediction horizons. It should be noted that the predictions and predictive powertrain controller are updated at 1 Hz, so the predictions that are shown do not show the full picture of the velocity predictions that were used to determine the optimal engine power. It should also be noted that for the V2V comparisons (Figure 33 and Figure 34) the predicted speeds are the same for the duration of the shorter prediction horizon. This is the case because of how the predictions are constructed for the V2V method. The lead vehicle information is used to identify the most similar cycle at that given time. Since we are seeking to see the impact of prediction horizon on engine operation, the same pattern recognition NN is used for both, thus the same lead vehicle information results in the same best match cycle identification that is used for the prediction.

In general, the engine operation is similar for the two different prediction horizons. Often, when the engine is on is the same, but the magnitudes vary in some instances. Figure 33 and Figure 34 depict situations where similar engine operation is seen, despite differences in prediction horizon and speed predictions. This behavior suggests that the prediction horizon alone does not often have a large impact on how the engine is operated. However, the ESS SOC also affects how the engine is operated. For instance, if there is a big difference in the SOC between the different prediction horizons, it will result in different engine operation, as shown in Figure 35.

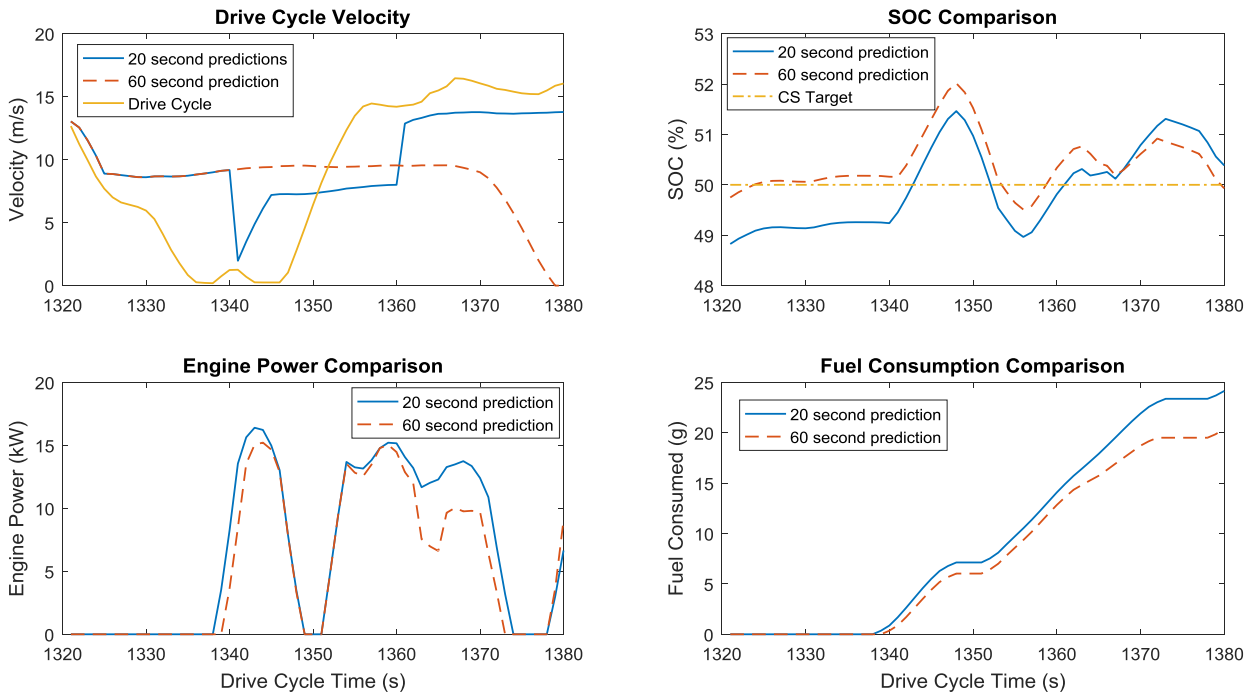

Figure 33: First example of similar engine operation in comparison of different prediction horizons

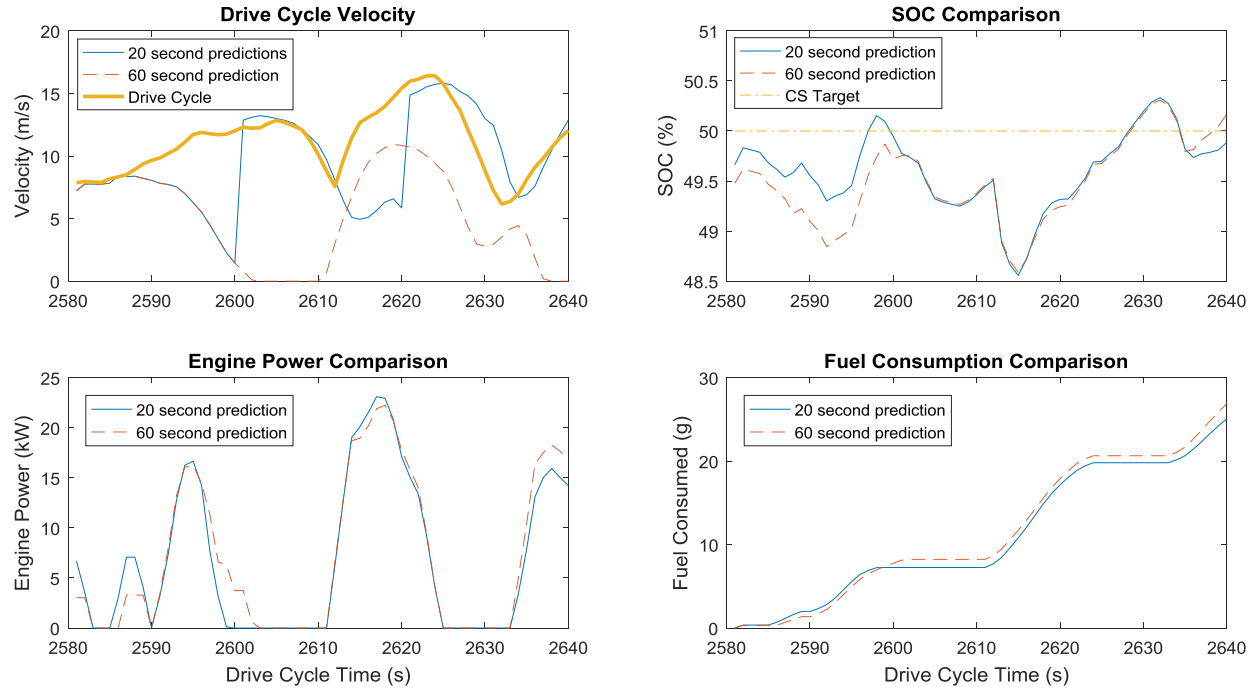

Figure 34: Second example of similar engine operation in comparison of different prediction horizons

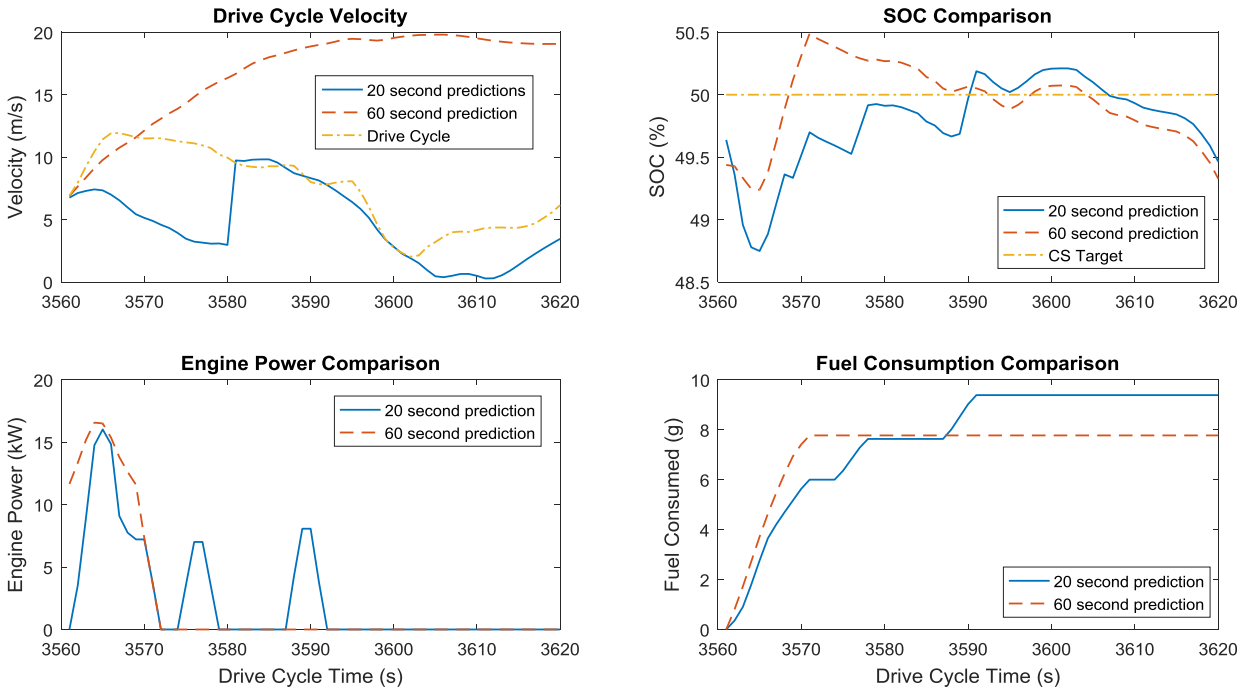

Figure 35: Example of shorter prediction horizon being forced to operate engine to meet predictive powertrain controller SOC CS constraints in comparison of different prediction horizons

The predictive powertrain controller aims at a charge-sustaining operation at the end of each prediction horizon. Thus, the shorter prediction horizons don't have as much flexibility for allowing the SOC to vary from the 50% CS SOC setpoint. The influence of this is depicted in Figure 36. It can be seen that the longer prediction horizon allows the SOC to vary more, and twice the shorter prediction horizon is forced to turn on the engine to maintain CS behavior.

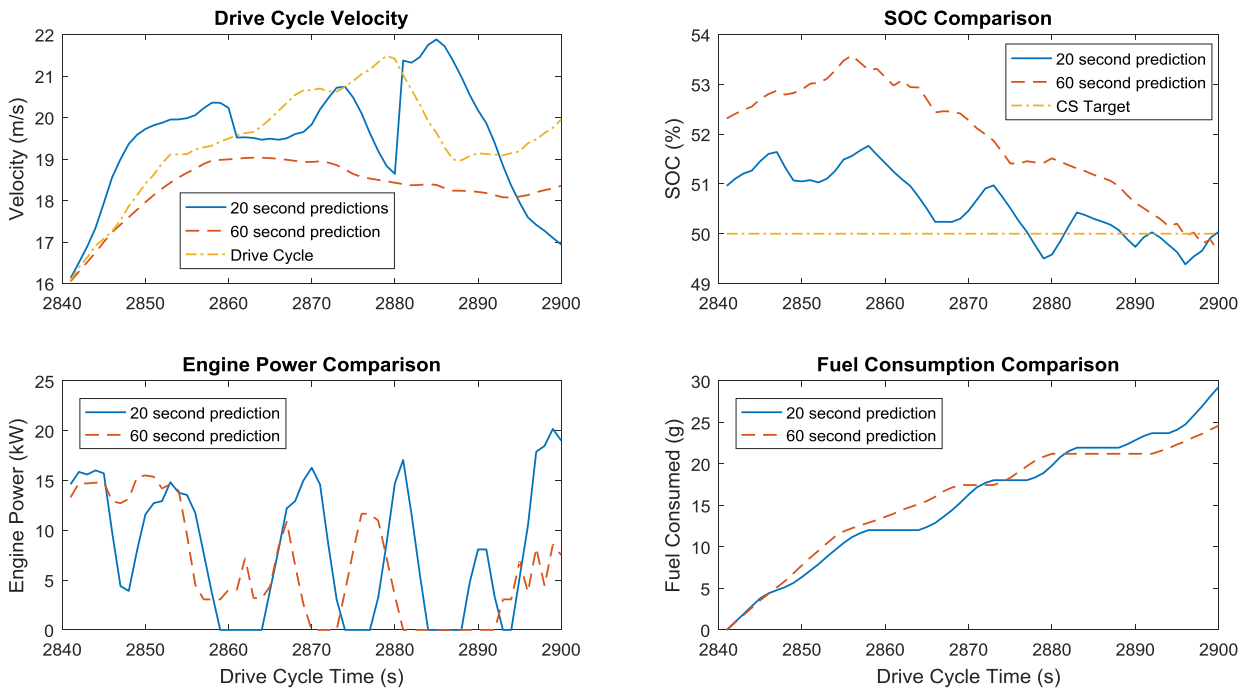

Figure 36: Example of different engine operation caused by different SOC values in comparison of different prediction horizons

To capture a more holistic view of the similarities of engine operation throughout a full drive cycle, the percent difference of engine power for the two prediction horizons was calculated, using Equation 5,

$$\%\, Difference = \frac{\left|P_{eng_{short}} - P_{eng_{long}}\right|}{\left(\frac{P_{eng_{short}} + P_{eng_{long}}}{2}\right)} * 100 \quad (5)$$

where $P_{eng_{short}}$ is the engine power for the 20-second prediction horizon and $P_{eng_{long}}$ is the engine power for the 60-second prediction horizon.

For the local prediction method on the combined cycle, 55% of the time the engine operation was within 5% of each other. If we look at only instances when at least one of the engines was operating (neglecting when both engines are off), 52% of the time the engine operation was within 50% difference. This indicates that engine on/off operation is very similar between the two

prediction horizons. When the engine is operated, the way in which it is operated, is still relatively similar. It should be noted that SOC differences are not isolated for this calculation, so different engine operations caused by SOC differences, such as that shown in Figure 36 impacts these calculations.

Likewise, for the V2V prediction horizon for the combined cycle, 65% of the time, the engine operation was within 5% of each other and when looking at only engine on periods, 67% of the time engine operations were within 50% of each other. These values likely are higher because the predictions are the exact same for the duration of the shorter prediction horizon, causing there to be more instances when the engine is operated alike. Overall, it seems that the optimal engine operation is not significantly impacted by the prediction horizon alone.

5. CONCLUSIONS

In this study we developed two methods of making future vehicle velocity predictions to be used to further understand if a shift from reactive to predictive EMS can be implemented with today's technology. The following section serves to answer the original research questions, restated here:

1. The quality and quantity of the driving prediction defines the tradeoff between prediction horizon duration and FE. What duration of prediction horizon realizes the largest FE improvement?
2. Are the FE benefits of prediction and optimal EMS robust to real-world variability in prediction error and drive cycles?
3. What level of FE can be realized through leveraging near-term low cost technologies, such as V2V?

5.1 TRADEOFFS BETWEEN PREDICTION HORIZON AND PREDICTION FIDELITY

In Chapter 2, we developed a vehicle speed prediction method using only currently-available, and on-vehicle technologies to investigate the tradeoff between fuel economy improvement and prediction fidelity. There is a competing relationship between prediction horizon length and prediction fidelity. Shorter prediction horizons produce predictions that are more accurate, but limit the FE benefit that the predictive powertrain controller can derive, as shorter prediction horizons do not obtain as much information. Conversely, longer prediction horizons provide more information to the predictive powertrain controller, but at the cost of prediction fidelity, as the predictions are more erroneous. Thus, the predictive powertrain controller will be optimizing

engine operation for speeds the vehicle may not actually travel. By understanding this tradeoff, we can determine the prediction horizon that balances these opposing forces.

For the local prediction method on the drive cycles investigated in this study, we conclude that 60-90 second prediction horizons result in the highest FE, achieving up to a 4.8% increase in CS MPGe over the baseline. For the V2V prediction method, the largest FE improvement was realized around the 120-second prediction horizon, resulting in up to a 6% increase in CS MPGe over the baseline. These represent the best balance between obtaining enough information for the predictive powertrain controller and producing accurate predictions to inform the predictive powertrain controller. Prediction horizons shorter than these are not obtaining enough information for the predicative powertrain controller to be able to realize as large FE improvements. Prediction horizons longer than this are too erroneous and the predictive powertrain controller will be optimizing for speeds vastly different from what the vehicle will actually drive.

5.2 ROBUSTNESS TO REAL-WORLD VARIABILITY

Before discussing the second research question, it is important to clarify the definition of robustness that in described in this study. In this context, we are defining robustness in terms of design robustness (or Taguchi robust design) [60] rather than robust control. In this, we want to understand if, even with variations, will the product – the prediction method and optimal EMS – still achieve its desired function – improving FE over the baseline. In this definition of robust design, the prediction and optimal EMS need to be able to achieve a FE improvement with variations that cannot be controlled, such as traffic, prediction error, NN training variations, etc.

Both prediction methods were developed and trained on real-world driving data, and FE simulations were completed with real-world driving data. Thus, prediction errors are real-world

prediction errors. All prediction horizons for each of the three individual cycles produced FE improvements over the baseline controller. This allows us to conclude prediction and optimal EMS are, indeed, robust to real-world prediction errors.

The three cycles that were simulated were along the same route, but driven at different times. The simulation results of the three drive cycles showed similar FE trends. This suggests that the prediction and optimal EMS are robust against real-world variability in drive cycles. However, further investigation into the impact of different lengths of drive cycles is needed, as the FE improvements for the combined cycle was reduced for all prediction horizons. However, this study suggests these speed prediction methods and EMS are robust real-world variability in the same drive cycle.

These prediction methods were able to achieve up to 85% of the maximum possible FE benefit while only utilizing technology that is commercial or near-term. This suggests that extremely accurate velocity predictions are not necessary to achieve real-world FE benefits and that any future information, even if erroneous, can be used to improve the FE of today's vehicles.

5.3 INCORPORATING NEAR-TERM TECHNOLOGIES FOR INCREASED FE

V2V communication was chosen to incorporate into a speed prediction method because it is a near-term and low cost technology. It is important to understand how near-term technologies can be utilized in the shift from reactive to predictive EMS. Additionally, the information of GPS location and vehicle speeds we assumed to be communicated between vehicles will be included in the first V2V communication systems. The V2V prediction method improved the viable prediction horizon range, as it consistently outperformed the local prediction method for prediction horizons greater than 60-90 seconds. It raised the FE improvement over baseline controller from the

maximum 4.8% improvement achieved by the local prediction to a maximum of 6% improvement when V2V was incorporated. Additionally, this prediction method produced predictions with a lower prediction RMSE mean and variance, as displayed in Figure 29. This study demonstrates that new technologies can be incrementally included into prediction and energy management strategies to continue to improve FE. However, we also conclude that current technology can be implemented into speed prediction methods to improve FE, and transition from reactive to predictive EMS.

5.4 FUTURE WORK

Several aspects of this study warrant further research to understand fully the impact of prediction error on FE improvement, as well as moving towards physical implementation. Investigating longer drive cycles would be insightful. The combined cycle resulted in a higher baseline FE, and also limited the FE improvement potential. Investigating different drive cycle lengths would allow for an understanding of the impact of drive cycle length on FE improvement potential. Additionally, a longer drive cycle should be investigated to further isolate sub-optimal FE results as being caused by prediction error. The drive cycle used in this study was convenient because many cycles need to be driven to gather training data for the prediction methods. However, a short drive cycle caused the ending SOC to have a significant impact on the FE of the drive cycle. A longer drive cycle would make the FE calculations less sensitive to the ending SOC.

The comparison between prediction methods for the 5-second prediction horizon suggest that the local prediction method produced predictions that were more similar to the actual vehicle velocity than the V2V method. As a result of this, it would be intriguing to modify the V2V prediction method by replacing the 5 seconds of V2V information with a locally predicted 5 second

prediction (from the NARX NN), and see if it would produce a larger FE improvement over the baseline. It would be interesting to compare this new combination of prediction methods with the V2V prediction method and see if the information obtained from the lead vehicle is actually improving FE.

Implementing these two prediction methods in the distance domain, rather than in the time domain, could potentially affect the FE improvement. It would be interesting to replicate this study, but shift everything from the time to distance domain. This could potentially improve the predictions, as issues such as stop light length, and variations between predicted and actual speed causing different distances to be traveled, would be corrected for. A similar investigation into the optimal prediction horizon (in distance) could be completed. A conclusion of whether predicting in the time or distance domain is superior could then be drawn.

Investigation into the sensitivity of prediction fidelity to the number of cycles in the drive cycle database and driving conditions captured in the training dataset could provide valuable insight into how many training cycles are needed to produce predictions with high enough fidelity to provide FE improvement. If more than eight drive cycles were included in the cycle database, would the prediction fidelity increase? As mentioned previously, all of the driving data in this study was taken during normal weather conditions. Studying the impact of poor weather on the prediction fidelity, as well as how many poor weather drive cycles in the training data set are needed to eliminate reduced prediction fidelity would be beneficial.

Many opportunities to improve the accuracy of the prediction methods exist. Incorporating more inputs into the NN, such as altitude, weather, or traffic data could produce more accurate predictions. Additionally, adding previous prediction error into the NARX NN would allow the NN to learn where it is producing highly erroneous predictions and use that to improve future

predictions. Adding in more information exchanged between the lead and ego vehicles, such as traffic or lead vehicle speed predictions could be used to increase prediction quality of the V2V prediction method.

In order to implement this prediction method into an actual vehicle, a predictive powertrain controller that is less computationally expensive is necessary. A controller that uses model predictive control, stochastic DP, or adaptive equivalent consumption minimization strategy would allow this to be run in real time [28], [45], [49]. The EcoCAR 3 Camaro would be an excellent platform to incorporate this in real-time after a real-time capable predictive powertrain controller is developed.

REFERENCES

[1] International_Energy_Organization, "CO2 emissions from fuel combustion," 2016.

[2] U.S. Environmental Protection Agency, "EPA and NHTSA Set Standards to Reduce Greenhouse Gases and Improve Fuel Economy for Model Years 2017-2025 Cars and Light Trucks," no. August 2012, pp. 1–10, 2012.

[3] J. Rogelj, M. den Elzen, N. Höhne, T. Fransen, H. Fekete, H. Winkler, R. Schaeffer, F. Sha, K. Riahi, and M. Meinshausen, "Paris Agreement climate proposals need a boost to keep warming well below 2 °C," *Nature*, vol. 534, no. 7609, pp. 631–639, 2016.

[4] A. E. Atabani, I. A. Badruddin, S. Mekhilef, and A. S. Silitonga, "A review on global fuel economy standards, labels and technologies in the transportation sector," *Renew. Sustain. Energy Rev.*, vol. 15, no. 9, pp. 4586–4610, 2011.

[5] U.S. Environmental Protection Agency, "Final Rule for Model Year 2017 and Later Light-Duty Vehicle Greenhouse Gas Emissions and Corporate Average Fuel Economy Standards." 2012.

[6] J. Romm, "The car and fuel of the future," *Energy Policy*, vol. 34, no. 17, pp. 2609–2614, 2006.

[7] T. H. Bradley and A. A. Frank, "Design, demonstrations and sustainability impact assessments for plug-in hybrid electric vehicles," *Renew. Sustain. Energy Rev.*, vol. 13, no. 1, pp. 115–128, 2009.

[8] M. A. Hannan, F. A. Azidin, and A. Mohamed, "Hybrid electric vehicles and their challenges: A review," *Renew. Sustain. Energy Rev.*, vol. 29, pp. 135–150, 2014.

[9] A. Jenn, I. L. Azevedo, and P. Ferreira, “The impact of federal incentives on the adoption of hybrid electric vehicles in the United States,” *Energy Econ.*, vol. 40, pp. 936–342, 2013.

[10] R. S. Levinson, D. K. Manley, and T. H. West, “History v. Simulation: An Analysis of the Drivers of Alternative Energy Vehicle Sales,” *SAE Int. J. Altern. Powertrains*, vol. 5, no. 2, pp. 2016-01–9142, 2016.

[11] Y. Ates, O. Erdinc, M. Uzunoglu, and B. Vural, “Energy management of an FC/UC hybrid vehicular power system using a combined neural network-wavelet transform based strategy,” *Int. J. Hydrogen Energy*, vol. 35, no. 2, pp. 774–783, 2010.

[12] Z. D. Asher, V. Wifvat, A. Navarro, S. Samuelsen, and T. H. Bradley, “The Importance of HEV Fuel Economy and Two Research Gaps Preventing Real World Implementation of Optimal Energy Management,” *SAE Tech. Pap.*, 2016.

[13] E. Ericsson, H. Larsson, and K. Brundell-Freij, “Optimizing route choice for lowest fuel consumption - Potential effects of a new driver support tool,” *Transp. Res. Part C Emerg. Technol.*, vol. 14, no. 6, pp. 369–383, 2006.

[14] F. Zhang, J. Xi, and R. Langari, “Real-Time Energy Management Strategy Based on Velocity Forecasts Using V2V and V2I Communications,” *IEEE Trans. Intell. Transp. Syst.*, pp. 1–15, 2016.

[15] M. A. M. Zulkefli, J. Zheng, Z. Sun, and H. X. Liu, “Hybrid powertrain optimization with trajectory prediction based on inter-vehicle-communication and vehicle-infrastructure-integration,” *Transp. Res. Part C Emerg. Technol.*, vol. 45, pp. 41–63, 2014.

[16] J. J. Valera, B. Heriz, G. Lux, J. Caus, and B. Bader, “Driving cycle and road grade on-

board predictions for the optimal energy management in EV-PHEVs," *2013 World Electr. Veh. Symp. Exhib. EVS 2014*, pp. 1–10, 2013.

[17] E. I. Vlahogianni, M. G. Karlaftis, and J. C. Golias, "Short-term traffic forecasting: Where we are and where we're going," *Transp. Res. Part C Emerg. Technol.*, vol. 43, pp. 3–19, 2014.

[18] X. Ma, Z. Tao, Y. Wang, H. Yu, and Y. Wang, "Long short-term memory neural network for traffic speed prediction using remote microwave sensor data," *Transp. Res. Part C Emerg. Technol.*, vol. 54, pp. 187–197, 2015.

[19] M. G. Karlaftis and E. I. Vlahogianni, "Statistical methods versus neural networks in transportation research: Differences, similarities and some insights," *Transp. Res. Part C Emerg. Technol.*, vol. 19, no. 3, pp. 387–399, 2011.

[20] Q. Gong, L. Yaoyu, and Z. Peng, "Power management of plug-in hybrid electric vehicles using neural network based trip modeling," in *American Control Conference, 2009*, 2009, pp. 4601–4606.

[21] A. Fotouhi, M. Montazeri-Gh, and M. Jannatipour, "Vehicle's velocity time series prediction using neural network," *Int. J. Automot. Eng.*, vol. 1, no. 1, pp. 21–28, 2011.

[22] I. Bosankic, L. Banjanovic-Mehmedovic, and F. Mehmedovic, "Speed profile prediction in intelligent transport systems exemplified by vehicle to vehicle interactions," *Cybern. Inf. Technol.*, vol. 15, no. 5, pp. 63–77, 2015.

[23] C. Sun, F. Sun, and H. He, "Investigating adaptive-ECMS with velocity forecast ability for hybrid electric vehicles," *Appl. Energy*, vol. 185, pp. 1644–1653, 2017.

[24] D. F. Opila, X. Wang, R. McGee, R. Brent Gillespie, J. A. Cook, and J. W. Grizzle, "Real-World Robustness for Hybrid Vehicle Optimal Energy Management Strategies Incorporating Drivability Metrics," *J. Dyn. Syst. Meas. Control*, vol. 136, no. 6, 2014.

[25] J. Jing, A. Kurt, E. Ozatay, J. Michelini, D. Filev, and U. Ozguner, "Vehicle Speed Prediction in a Convoy Using V2V Communication," *IEEE Conf. Intell. Transp. Syst. Proceedings, ITSC*, vol. 2015–Octob, pp. 2861–2868, 2015.

[26] E. Ericsson, "Variability in urban driving patterns," *Transp. Res. Part D Transp. Environ.*, vol. 5, pp. 337–354, 2000.

[27] Q. Gong, Y. Li, and Z.-R. Peng, "Trip based optimal power management of plug-in hybrid electric vehicles using gas-kinetic traffic flow model," in *2008 American Control Conference*, 2008, pp. 3225–3230.

[28] M. A. M. Zulkefli and Z. Sun, "Real-time Powertrain Optimization Strategy for Connected Hybrid Electrical Vehicle," in *ASME 2016 Dynamic Systems and Control Conference*, 2017, pp. 1–10.

[29] Y. He, M. Chowdhury, P. Pisu, and Y. Ma, "An energy optimization strategy for power-split drivetrain plug-in hybrid electric vehicles," *Transp. Res. Part C Emerg. Technol.*, vol. 22, pp. 29–41, 2012.

[30] L. Fu, U. Ozguner, P. Tulpule, and V. Marano, "Real-time energy management and sensitivity study for hybrid electric vehicles," in *American Control Conference (ACC), 2011*, 2011, pp. 2113–2118.

[31] F. A. Bender, M. Kaszynski, and O. Sawodny, "Drive Cycle Prediction and Energy

Management Optimization for Hybrid Hydraulic Vehicles," *IEEE Trans. Veh. Technol.*, vol. 62, no. 8, pp. 3581–3592, 2013.

[32] Z. D. Asher, T. Cummings, and T. H. Bradley, "The Effect of Hill Planning and Route Type Identification Prediction Signal Quality on Hybrid Vehicle Fuel Economy," 2016.

[33] A. Rezaei and J. B. Burl, "Effects of Time Horizon on Model Predictive Control for Hybrid Electric Vehicles," in *International Federation of Automatic Control*, 2015, vol. 48, no. 15, pp. 252–256.

[34] C. Sun, S. J. Moura, X. Hu, J. K. Hedrick, and F. Sun, "Dynamic Traffic Feedback Data Enabled Energy Management in Plug-in Hybrid Electric Vehicles," *IEEE Trans. Control Syst. Technol.*, vol. 23, no. 3, pp. 1075–1086, May 2015.

[35] R. Bellman, "Dynamic Programming and Lagrange Multipliers.," *Proc. Natl. Acad. Sci. U. S. A.*, vol. 42, no. 10, pp. 767–769, 1956.

[36] A. Sciarretta and L. Guzzella, "Control of hybrid electric vehicles," *IEEE Control Syst. Mag.*, vol. 27, no. 2, pp. 60–70, Apr. 2007.

[37] O. Sundström and L. Guzzella, "A generic dynamic programming Matlab function," *Proc. IEEE Int. Conf. Control Appl.*, no. 7, pp. 1625–1630, 2009.

[38] S. E. Lyshevski and C. Yokomoto, "Control of Hybrid Electric Vehicles," *Control*, no. June, 1998.

[39] A. Brahma, Y. Guezennec, and G. Rizzoni, "Optimal energy management in series hybrid electric vehicles," in *Proceedings of the 2000 American Control Conference. ACC (IEEE Cat. No.00CH36334)*, 2000, vol. 1, no. 6, pp. 60–64 vol.1.

[40] C.-C. Lin, J.-M. Kang, J. W. Grizzle, and H. Peng, "Energy management strategy for a parallel hybrid electric truck," *Am. Control Conf. 2001. Proc. 2001*, vol. 4, no. D, pp. 2878–2883 vol.4, 2001.

[41] R. Rajamani, *Vehicle Dynamics and Control*, Second. Springer, 2006.

[42] K. J. de Jager B, van Keulen T, *Optimal Control of Hybrid Vehicles*. 2013.

[43] P. Zhang, F. Yan, and C. Du, "A comprehensive analysis of energy management strategies for hybrid electric vehicles based on bibliometrics," *Renew. Sustain. Energy Rev.*, vol. 48, pp. 88–104, Aug. 2015.

[44] S. J. Moura, H. K. Fathy, D. S. Callaway, and J. L. Stein, "A Stochastic Optimal Control Approach for Power Management in Plug-In Hybrid Electric Vehicles," *IEEE Trans. Control Syst. Technol.*, vol. 19, no. 3, pp. 545–555, May 2011.

[45] D. F. Opila, X. Wang, R. McGee, and J. W. Grizzle, "Real-Time Implementation and Hardware Testing of a Hybrid Vehicle Energy Management Controller Based on Stochastic Dynamic Programming," *J. Dyn. Syst. Meas. Control*, vol. 135, no. March 2013, pp. 21002-1-21002–11, 2012.

[46] Y. Wang and Z. Sun, "SDP-based extremum seeking energy management strategy for a power-split hybrid electric vehicle," *Am. Control Conf.*, pp. 553–558, 2012.

[47] S. J. Moura, J. L. Stein, and H. K. Fathy, "Battery-health conscious power management in plug-in hybrid electric vehicles via electrochemical modeling and stochastic control," *IEEE Trans. Control Syst. Technol.*, vol. 21, no. 3, pp. 679–694, 2013.

[48] H. Borhan, A. Vahidi, A. M. Phillips, M. L. Kuang, I. V. Kolmanovsky, and S. Di Cairano,

"MPC-based energy management of a power-split hybrid electric vehicle," *IEEE Trans. Control Syst. Technol.*, vol. 20, no. 3, pp. 593–603, 2012.

[49] S. Di Cairano, D. Bernardini, A. Bemporad, and I. V. Kolmanovsky, "Stochastic MPC With Learning for Driver-Predictive Vehicle Control and its Application to HEV Energy Management," *IEEE Trans. Control Syst. Technol.*, vol. 22, no. 3, pp. 1018–1031, May 2014.

[50] F. Yan, J. Wang, and K. Huang, "Hybrid electric vehicle model predictive control torque-split strategy incorporating engine transient characteristics," *IEEE Trans. Veh. Technol.*, vol. 61, no. 6, pp. 2458–2467, 2012.

[51] P. Poramapojana and B. Chen, "Minimizing HEV fuel consumption using model predictive control," *Proc. 2012 IEEE/ASME 8th IEEE/ASME Int. Conf. Mechatron. Embed. Syst. Appl.*, pp. 148–153, 2012.

[52] L. He, T. Shen, L. Yu, N. Feng, and J. Song, "A model-predictive-control-based torque demand control approach for parallel hybrid powertrains," *IEEE Trans. Veh. Technol.*, vol. 62, no. 3, pp. 1041–1052, 2013.

[53] T. Cummings, Z. D. Asher, and T. H. Bradley, "The Effect of Trip Preview Prediction Signal Quality on Hybrid Vehicle Fuel Economy," in *4th IFAC Workshop on Engine and Powertrain Control Simulation and Modeling (E-COSM 2015)*, 2015.

[54] A. N. Laboratory, "2010 Toyota Prius | Argonne National Laboratory." [Online]. Available: www.anl.gov/energy-systems/group/downloadable-dynamometer-database/hybrid-electric-vehicles/2010-toyota-prius.

[55] M. H. Beale, M. T. Hagan, and H. B. Demuth, "Neural Network Toolbox ™ Getting Started Guide How to Contact MathWorks," 2015.

[56] "V2V Safety Technology Now Standard on Cadillac CTS Sedans," 2017. [Online]. Available: https://www.gm.com/mol/m-2017-mar-0309-v2v.html. [Accessed: 07-Jul-2017].

[57] IEEE, "First Toyota cars to include V2V and V2I communication by the end of 2015," 2015. [Online]. Available: http://sites.ieee.org/connected-vehicles/2015/09/30/first-toyota-cars-to-include-v2v-and-v2i-communication-by-the-end-of-2015/. [Accessed: 07-Jul-2017].

[58] USDOT, "NHTSA Issues Notice of Proposed Rulemaking and Research Report on Vehicle-To-Vehicle Communications," pp. 1–4, 2016.

[59] M. F. Møller, "A scaled conjugate gradient algorithm for fast supervised learning," *Neural Networks*, vol. 6, no. 4, pp. 525–533, 1993.

[60] G. Taguchi, "Taguchi on robust technology development: bringing quality engineering upstream," *Am. Soc. Mech. Eng.*, 1993.

APPENDIX

1. SUPPLEMENTAL PLOTS FOR PREDICTION METHOD RMSE COMPARISON

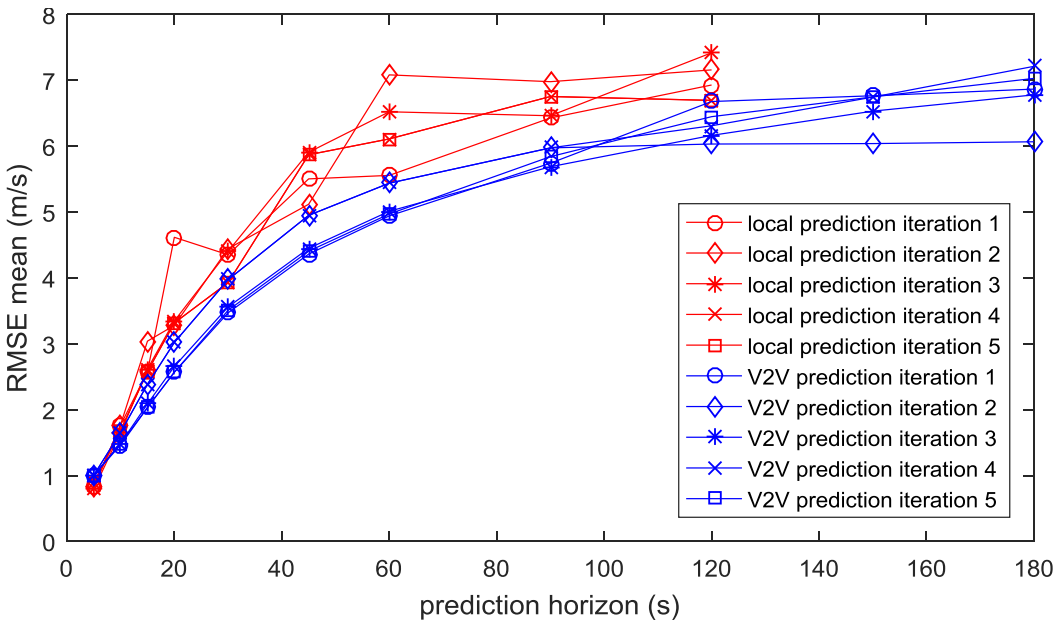

Figure 37: Comparison between local and V2V prediction methods via RMSE mean of all predictions from cycle 2

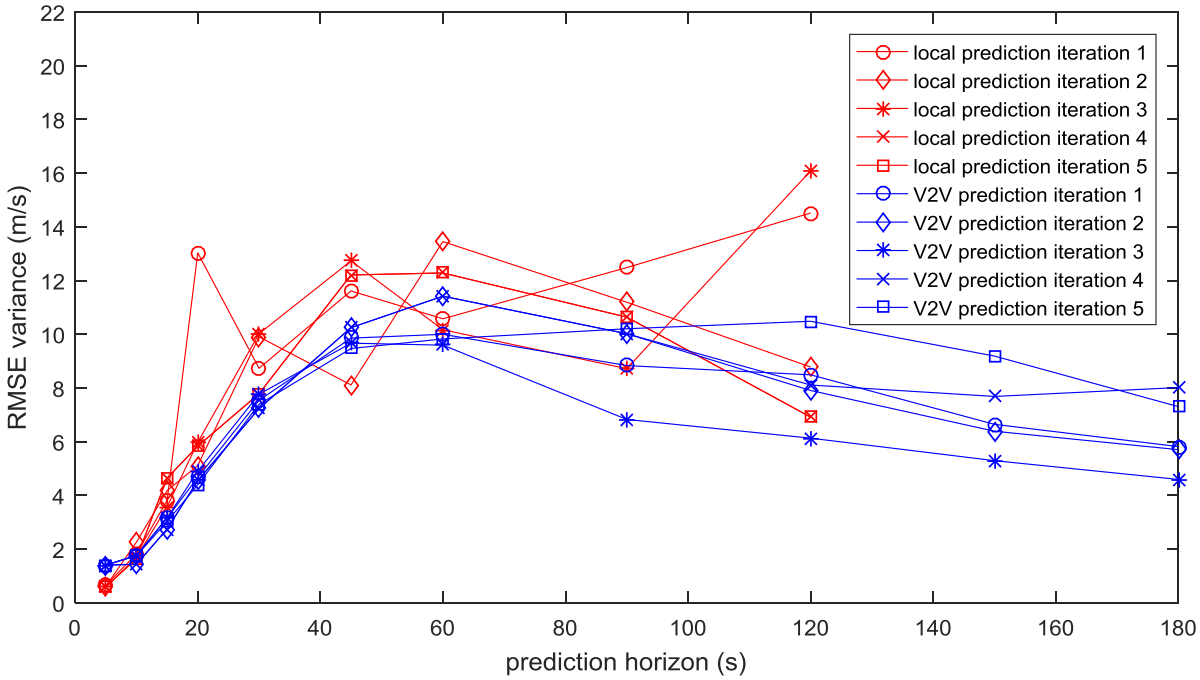

Figure 38: Comparison between local and V2V prediction methods via RMSE variance of all predictions from cycle 2

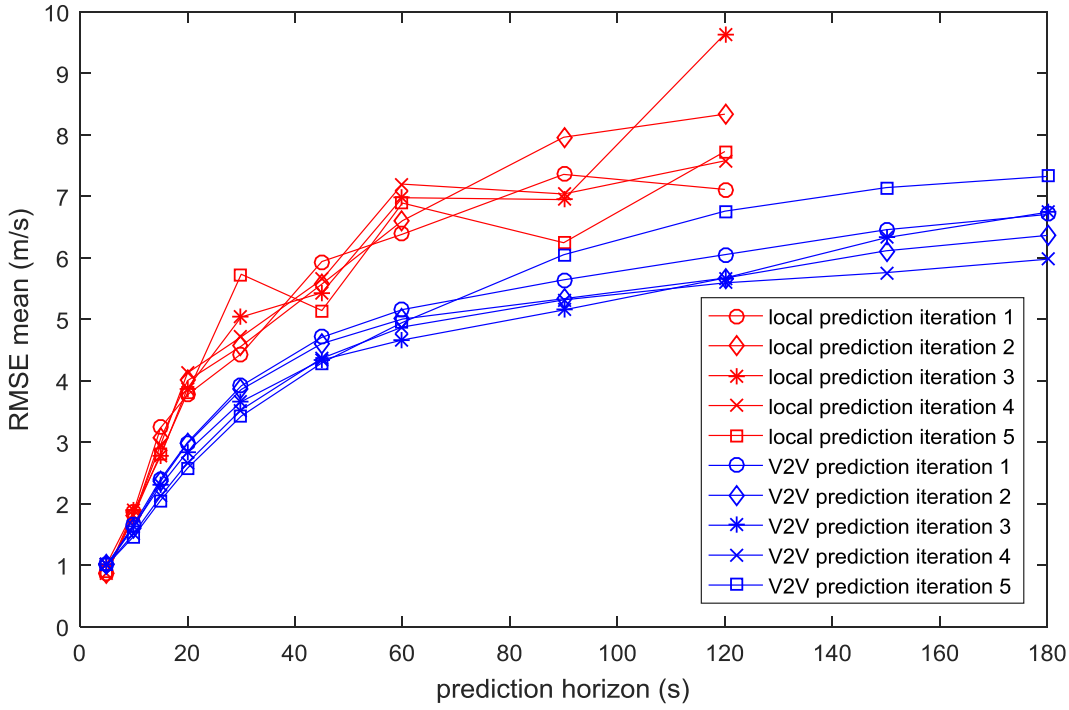

Figure 39: Comparison between local and V2V prediction methods via RMSE mean of all predictions from cycle 3

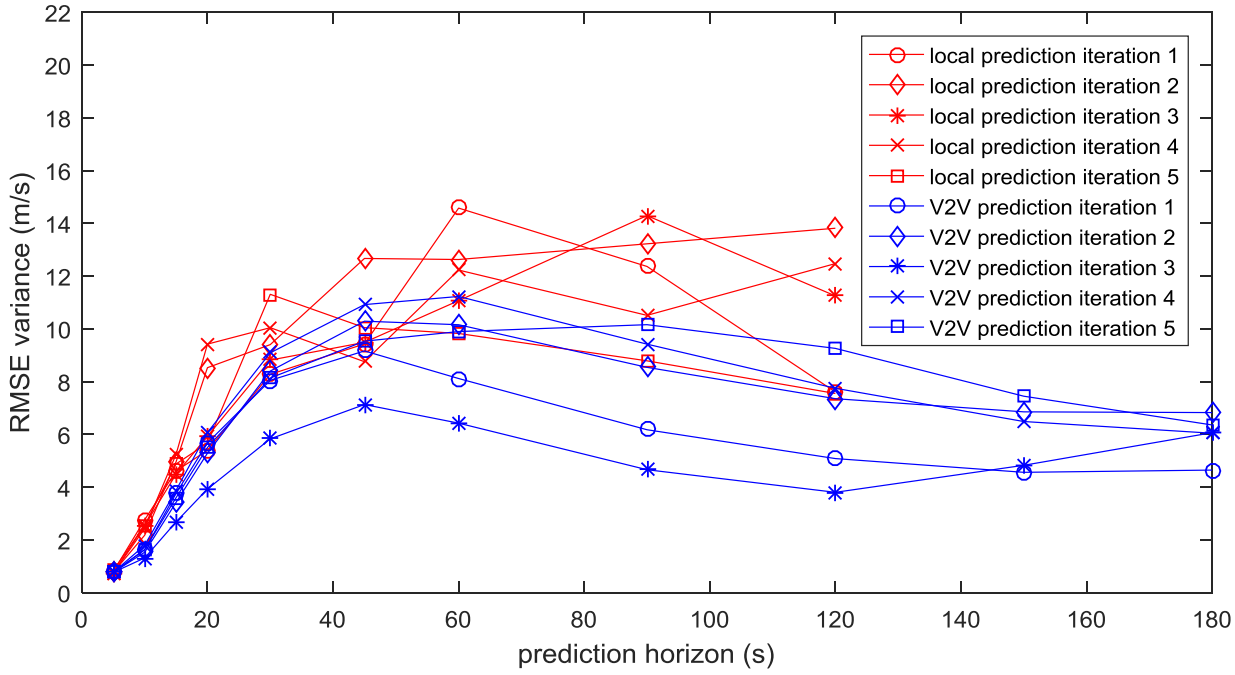

Figure 40: Comparison between local and V2V prediction methods via RMSE variance of all predictions from cycle 3

2. SUPPLEMENTAL PLOTS FOR COMPARISON OF 5-SECOND PREDICTION HORIZON

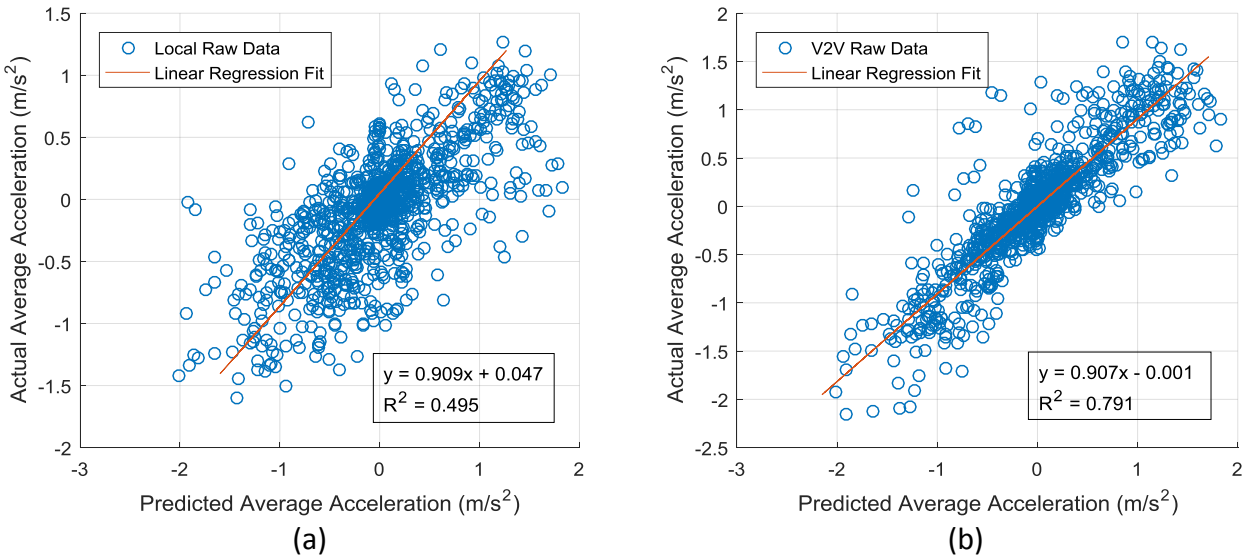

Figure 41: Comparison of predicted and actual vehicle accelerations with linear regression provides insight into why the local prediction method (a) realizes a larger FE benefit than the V2V prediction method (b) for 5-second prediction window on cycle 3

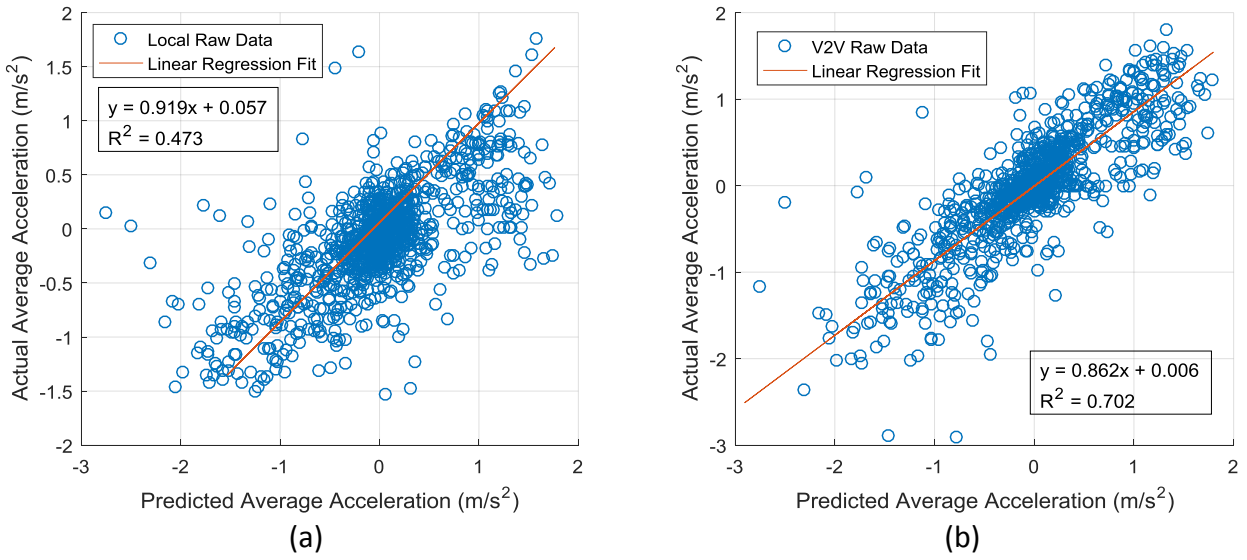

Figure 42: Comparison of predicted and actual vehicle accelerations with linear regression provides insight into why the local prediction method (a) realizes a larger FE benefit than the V2V prediction method (b) for 5-second prediction window on cycle 3